Stony Brook University | The State University of New York

INT program: Intersection of nuclear structure and high-energy nuclear collisions

Isobar collisions as precision nuclear structure probes

Jiangyong Jia

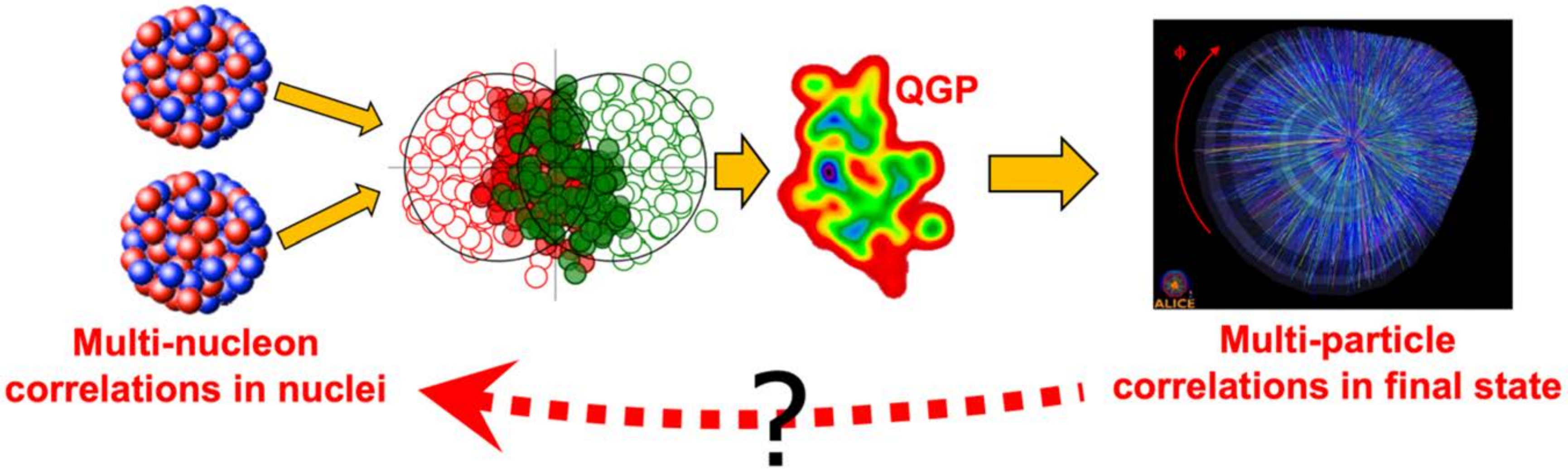

Landscape of nuclear physics

Quark-gluon plasma

hadrons

nuclei

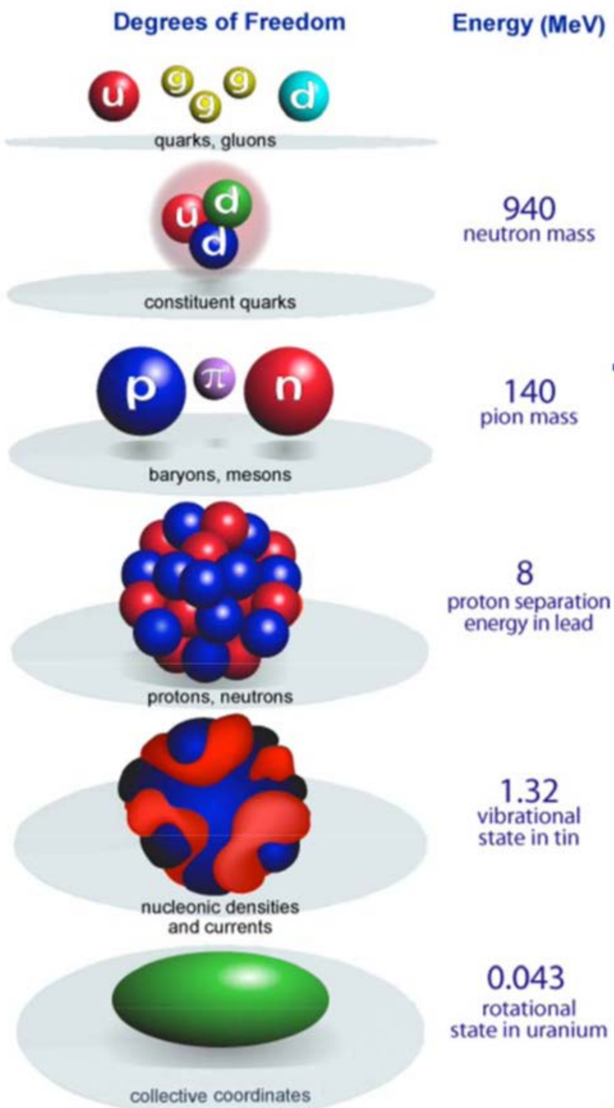

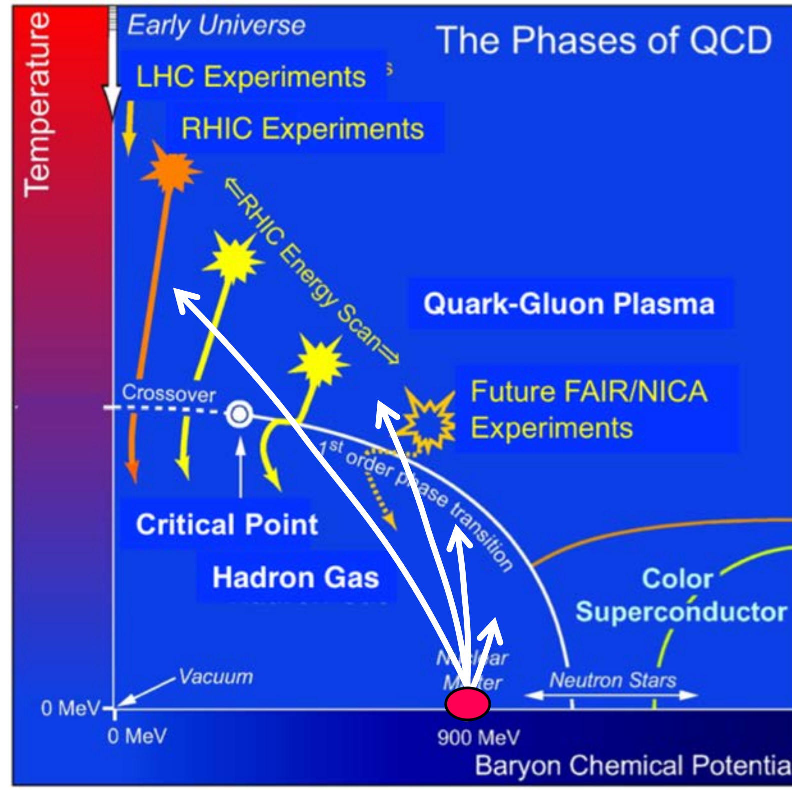

Most nuclear experiments starts with nuclei

Rich structure of atomic nuclei

- Collective phenomena of many-body quantum system
  - clustering, halo, skin, bubble…
  - quadrupole/octupole/hexdecopole deformations
  - Nontrivial evaluation with N and Z.

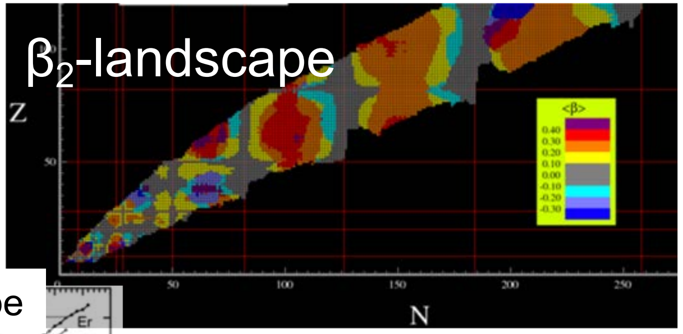

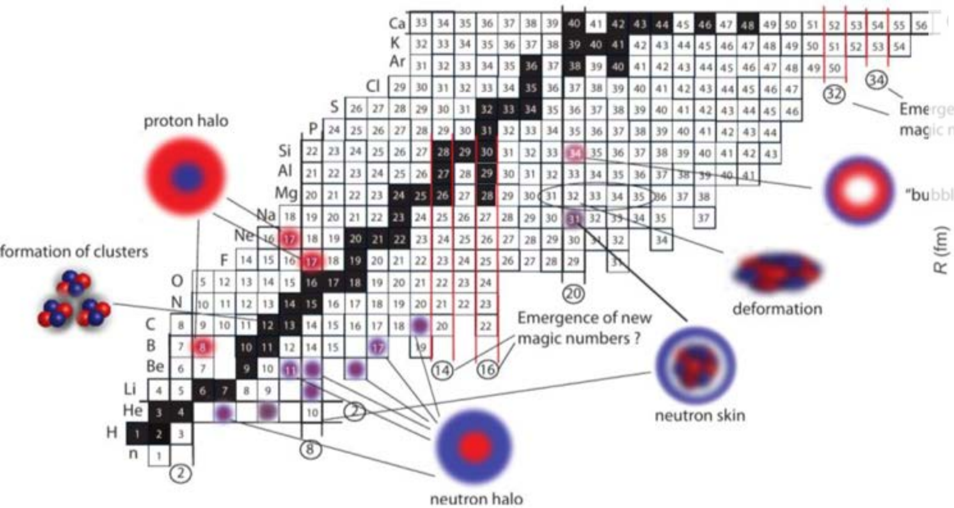

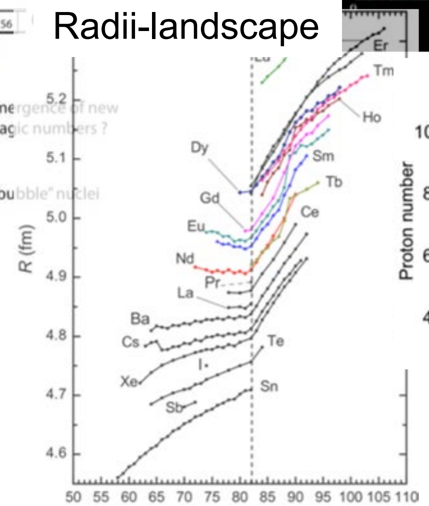

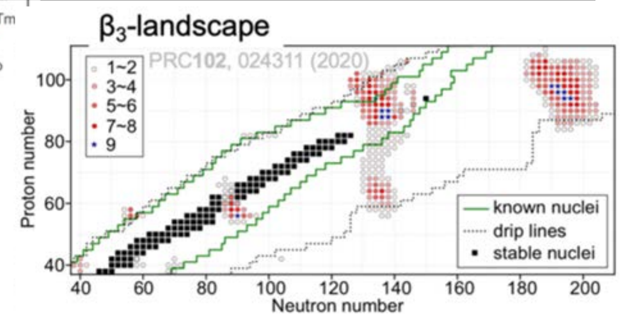

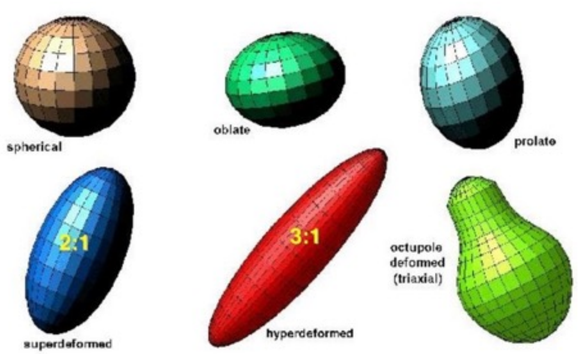

- Understanding via effective nuclear theories
  - Lattice, Ab.initio (starting from NN interaction)
  - Shell models (configuration interaction)
  - DFT models (non-relativistic and covariant)

Collective structure for heavy ion collision

$$\rho(r,\theta,\phi) = \frac{\rho_0}{1 + e^{(r - R(\theta,\phi))/a_0}}$$

$$R(\theta,\phi) = R_0\left(1 + \beta_2[\cos\gamma Y_{2,0} + \sin\gamma Y_{2,2}] + \beta_3 \sum_{m=-3}^{3} \alpha_{3,m} Y_{3,m} + \beta_4 \sum_{m=-4}^{4} \alpha_{4,m} Y_{4,m}\right)$$

Quadrupole:

Triaxiality:

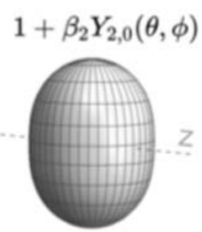

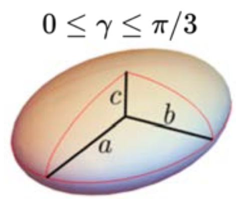

Radial distributions, R_0, a_0:

Octupole:

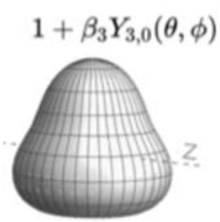

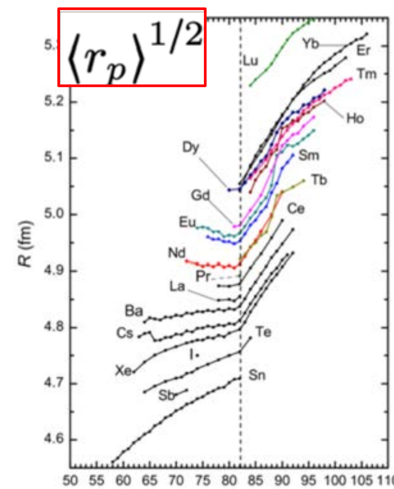

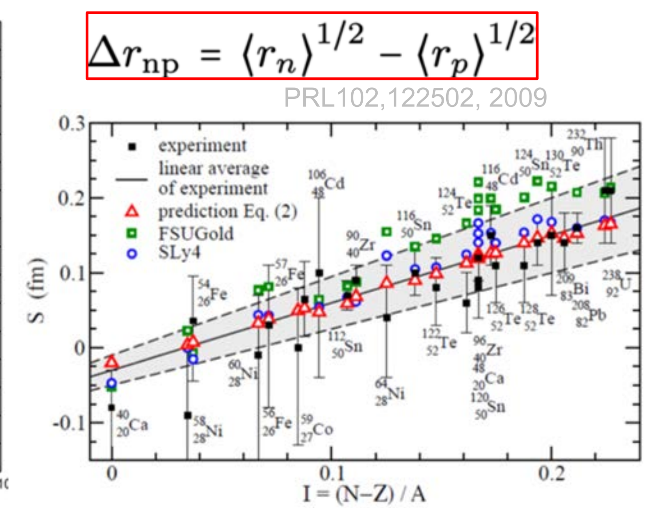

Hexadecapole:

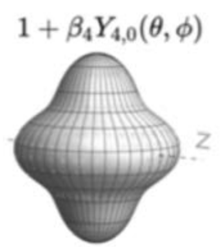

-

High-energy heavy ion collision

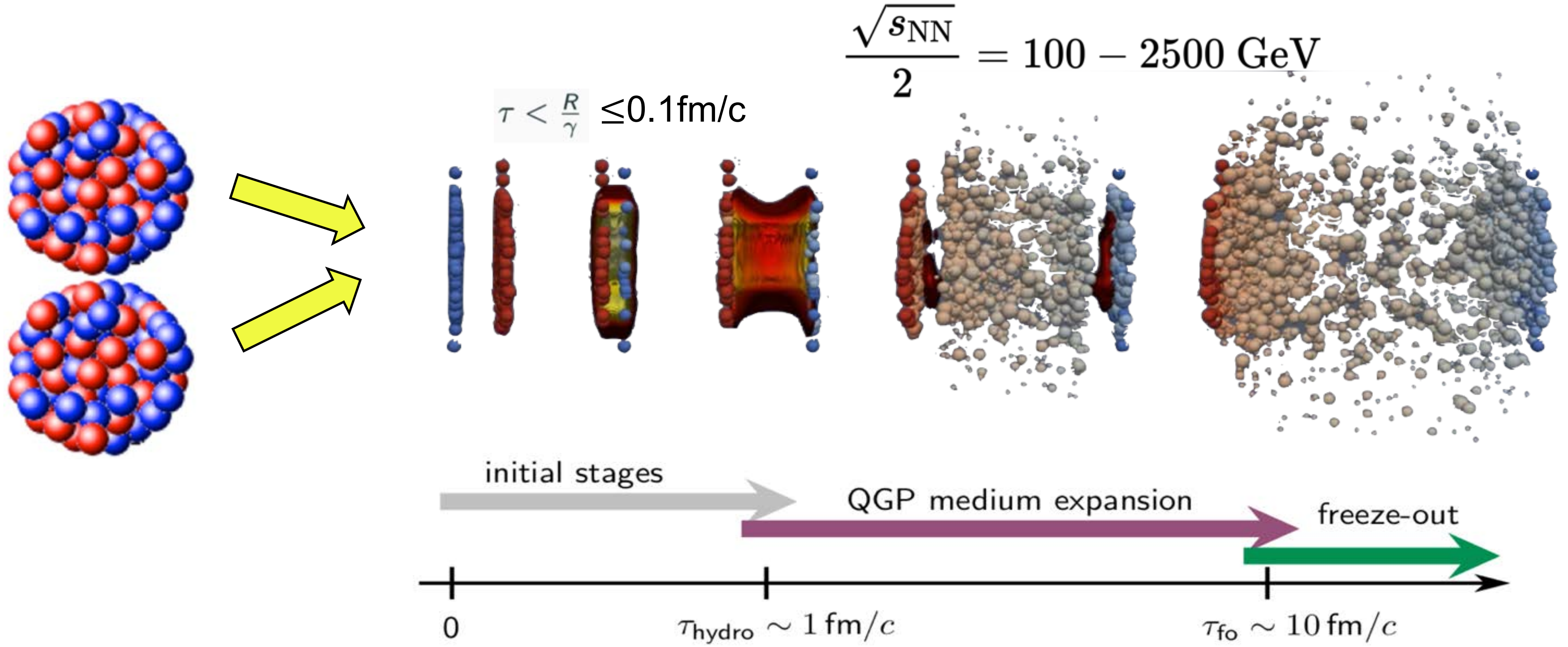

400 nucleons → 30000 hadrons

in 10^{-23} seconds

Key features facilitating the connection to nuclear structure 1) Extremely short passing time means that collision takes a snap-shot of the nuclear and nucleon wavefunction in the two nuclei. 2) Large particle production in overlap region means the produced QGP is dense and expand hydrodynamically.

Outline

Nuclear structure | Initial condition | Final state

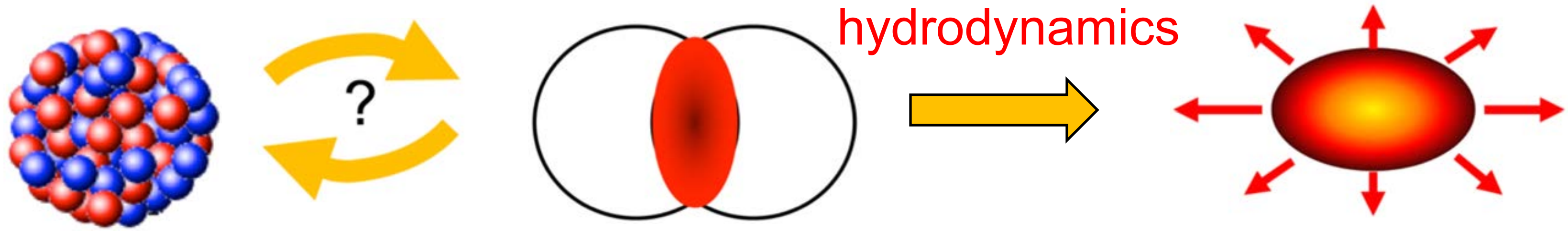

Shape and radial dis. | Volume, size and shape | observables

$\beta_2 \rightarrow$ Quadrupole deformation
$\beta_3 \rightarrow$ Octupole deformation
$a_0 \rightarrow$ Surface diffuseness
$R_0 \rightarrow$ Nuclear size

N_{part}

$R_{\perp}^2 \propto \langle r_{\perp}^2 \rangle,$

$\mathcal{E}_n \propto \langle r_{\perp}^n e^{in\phi} \rangle$

$$\frac{d^2N}{d\phi dp_T} = N(p_T)\left(\sum_n V_{\rm n}\, e^{-in\phi}\right)$$

- Describe hydrodynamics that connects initial condition and final state.
- Describe observables used to infer QGP properties and the initial condition
- Discuss how nuclear structure impacts the initial condition and observables
- Case study with isobar collision data to imagine both IC and NS.
- Speculate future system scan and its prospect for nuclear structure imaging.

Hydrodynamic evolution

Relativistic viscous Hydrodynamics (first-order):

Energy-momentum conservation

$$\partial_\mu T^{\mu\nu} = 0$$

$$T^{\mu\nu} = \epsilon u^\mu u^\nu - (P + \Pi)\Delta^{\mu\nu} + \pi^{\mu\nu}$$

Equation-of-state P(∈) Bulk pressure Shear tensor

$$\pi^{\mu\nu} = -\eta\sigma^{\mu\nu}$$ η: shear viscosity

$$\Pi = -\zeta\nabla^{\perp}_{\lambda}u^\lambda$$ ζ : bulk viscosity

1) Collective flow driven by QCD eos: $F = -\nabla P(\epsilon)$

2) But resisted by viscosity

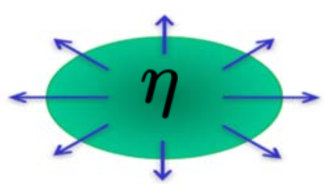

Reduce anisotropic flow

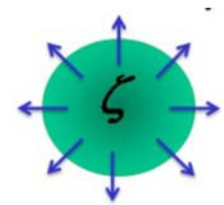

Reduce radial flow

Shape-flow transmutation via pressure-gradient force

Initial condition

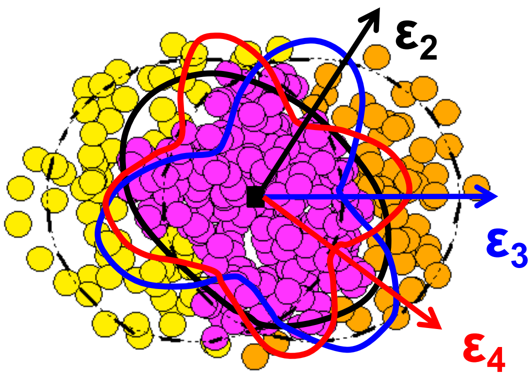

$$F = -\nabla P(\epsilon)$$

Hydro-response

Final Particle flow

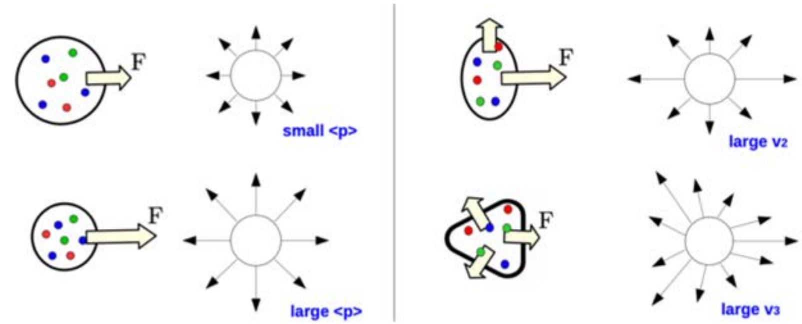

volume, size and shape

$N_{\rm part}$ $\quad R_\perp^2 \propto \langle r_\perp^2 \rangle,$

$$\mathcal{E}_2 \propto \left\langle r_\perp^2 e^{i2\phi} \right\rangle$$
$$\mathcal{E}_3 \propto \left\langle r_\perp^3 e^{i3\phi} \right\rangle \quad \mathcal{E}_n \propto \langle r_\perp^n Y_{n,n} \rangle$$
$$\mathcal{E}_4 \propto \left\langle r_\perp^4 e^{i4\phi} \right\rangle$$
$$\cdots$$

Multiplicity Radial Flow Harmonic Flow

N_{ch}

$$\frac{d^2N}{d\phi dp_T} = N(p_T)\left(\sum_n V_n\, e^{-in\phi}\right)$$

arXiv:1206.1905

Advantage of High energy:
⇒Large multiplicity and boost invariance
⇒approx. linear response in each event

$$N_{ch} \propto N_{part} \quad \frac{\delta[p_T]}{[p_T]} \propto -\frac{\delta R_\perp}{R_\perp} \quad V_n \propto \mathcal{E}_n$$

Shape-flow transmutation via pressure-gradient force

Initial condition

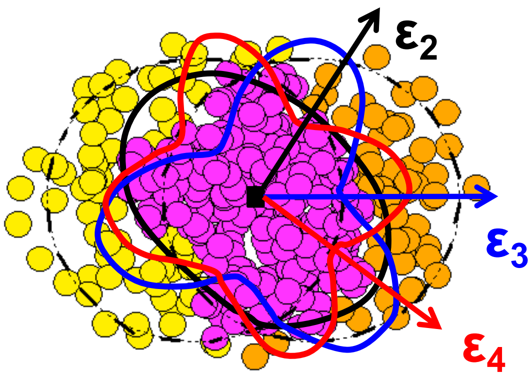

$$F = -\nabla P(\epsilon)$$

Hydro-response

Final Particle flow

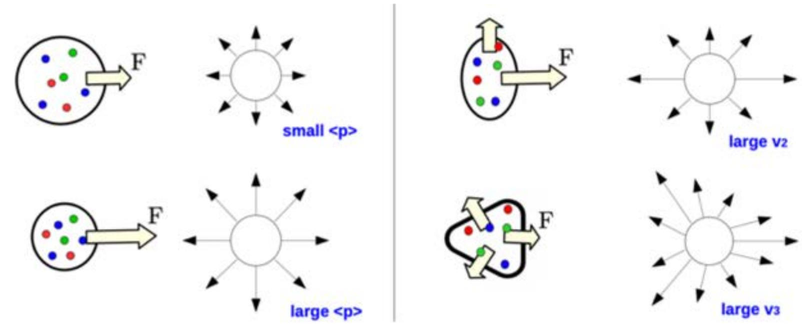

volume, size and shape

N_{part} $\quad R_\perp^2 \propto \langle r_\perp^2 \rangle,$

$$\mathcal{E}_2 \propto \left\langle r_\perp^2 e^{i2\phi} \right\rangle$$
$$\mathcal{E}_3 \propto \left\langle r_\perp^3 e^{i3\phi} \right\rangle$$
$$\mathcal{E}_4 \propto \left\langle r_\perp^4 e^{i4\phi} \right\rangle$$

...

Multiplicity Radial Flow Harmonic Flow

N_{ch} $\quad \dfrac{d^2N}{d\phi dp_T} = N(p_T)\left(\sum_n V_n\, e^{-in\phi}\right)$

Radial flow

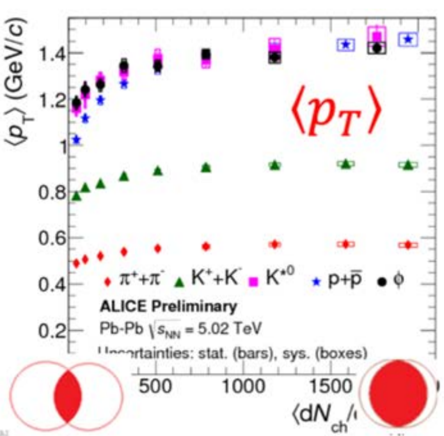

Elliptic flow

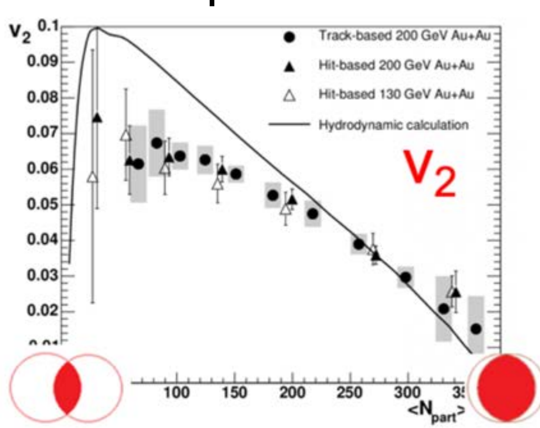

- Collective expansion for small Knudson number $\frac{\lambda}{R} \ll 1$
- Viscosity effects amplified by velocity gradient $\pi^{\mu\nu} = -\eta\sigma^{\mu\nu}$
- For flow to develop quickly, η/s must be small

$$\frac{\eta}{s} \sim 1-3\times\frac{1}{4\pi}\frac{\hbar}{k}$$

Richness of flow fluctuations

One big-bang event

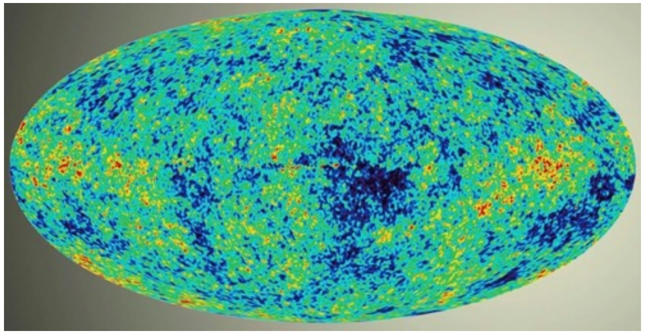

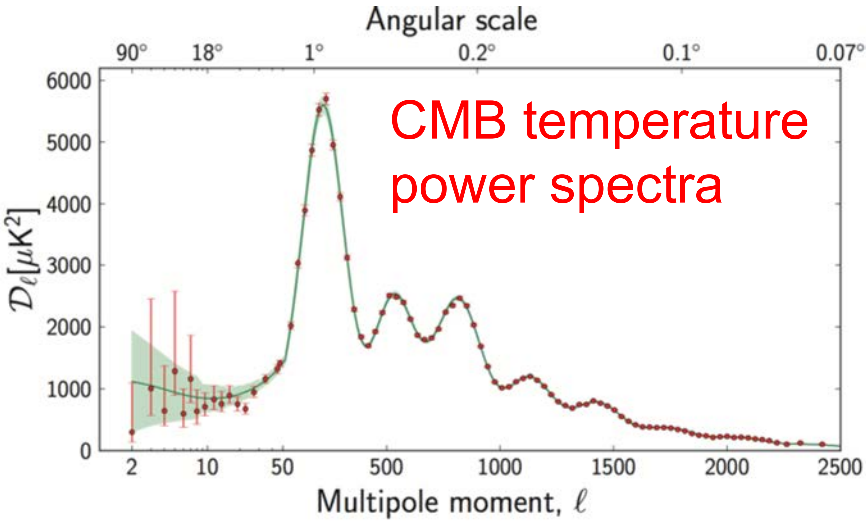

CMB temperature power spectra

Many little-bang events

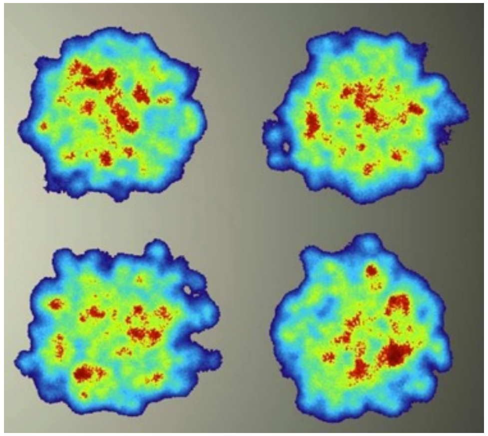

$$p(\boldsymbol{V}_2, \boldsymbol{V}_3 \ldots) = \frac{1}{N_{\mathrm{evts}}} \frac{dN_{\mathrm{evts}}}{d\boldsymbol{V}_2 d\boldsymbol{V}_3 \ldots}$$

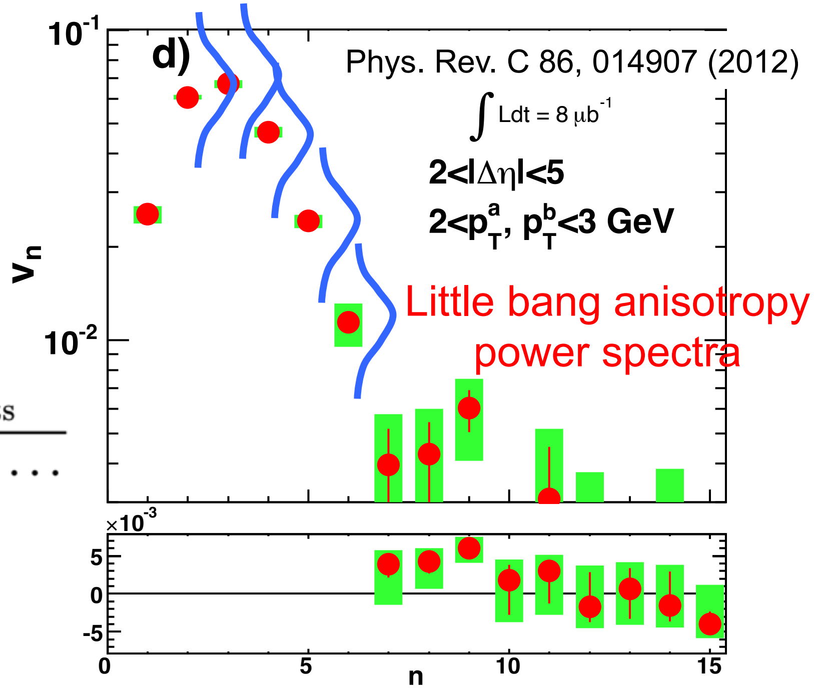

Little bang anisotropy power spectra

Observables for flow fluctuations

- Single particle distribution

Flow vector: $\boldsymbol{V}_n = v_n e^{in\Psi_n}$

$$\frac{d^2N}{d\phi dp_{\mathrm{T}}} = N(p_T)\left[1 + 2\sum_n v_{\mathrm{n}}(p_T)\cos n(\phi - \Psi_n(p_T))\right]$$
$$= N(p_T)\left[\sum_{n=-\infty}^{\infty} V_{\mathrm{n}}(p_T)e^{in\phi}\right]$$

Radial flow

Anisotropic flow

- Two-particle correlation function

$$\left\langle \frac{d^2N_1}{d\phi dp_{\mathrm{T}}}\frac{d^2N_2}{d\phi dp_{\mathrm{T}}}\right\rangle \Rightarrow \langle \boldsymbol{V}_n(p_{T1})\boldsymbol{V}_n^*(p_{T2})\rangle \quad n - n = 0$$

- Multi-particle correlation function

These multi-particle observables quantifies the initial volume, size and shape event-by-event

$$\left\langle \frac{d^2N_1}{d\phi dp_{\mathrm{T}}} \cdots \frac{d^2N_m}{d\phi dp_{\mathrm{T}}}\right\rangle \Rightarrow \left\langle V_{n_1}V_{n_2}...V_{n_m}\right\rangle \quad n_1 + n_2 + ... + n_m = 0$$

$$\downarrow$$

$$p(\boldsymbol{V}_2, \boldsymbol{V}_3 \ldots) = \frac{1}{N_{\mathrm{evts}}}\frac{dN_{\mathrm{evts}}}{d\boldsymbol{V}_2 d\boldsymbol{V}_3 \ldots}$$

Observables for flow fluctuations

E-by-E flow amplitude distribution $p(v_n)$

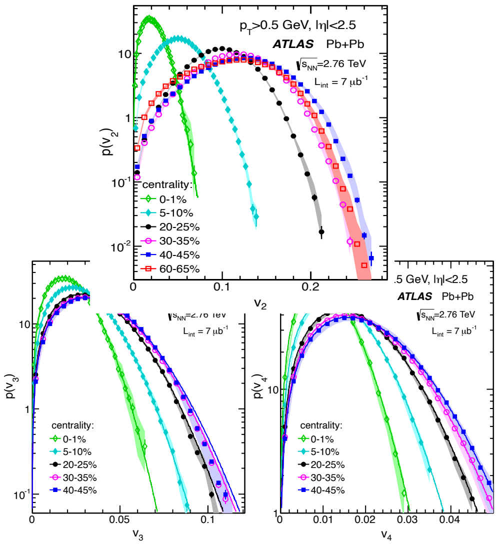

Event-plane correlation $p(\Psi_n,\Psi_m,\Psi_k)$

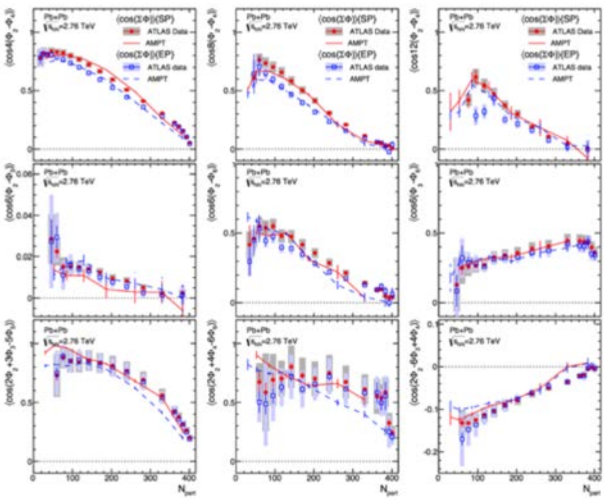

v_n amplitude correlation $p(v_n,v_m)$

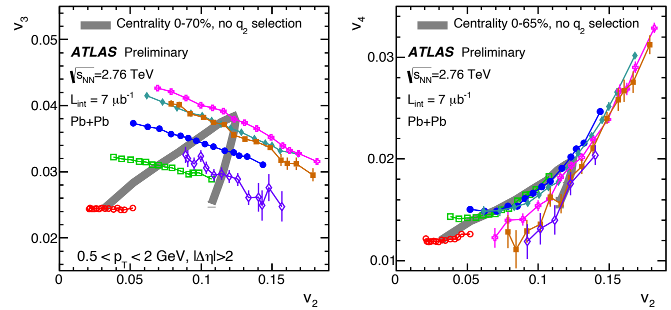

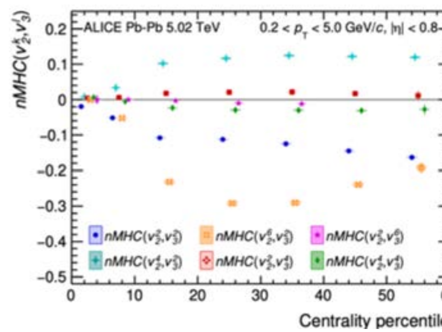

Higher-harmonics v_2-v_6

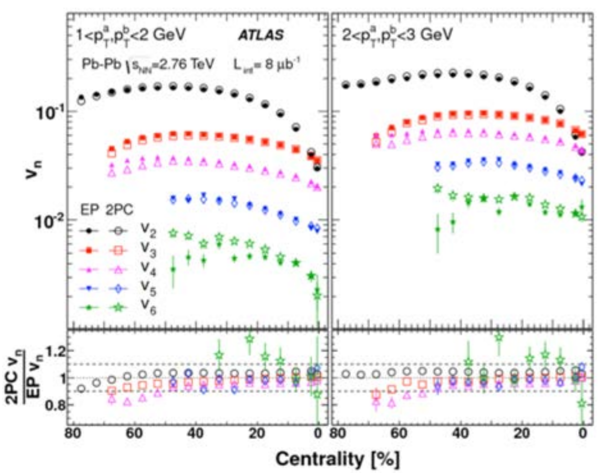

v_n-p_T correaltion $p(v_n, p_T)$

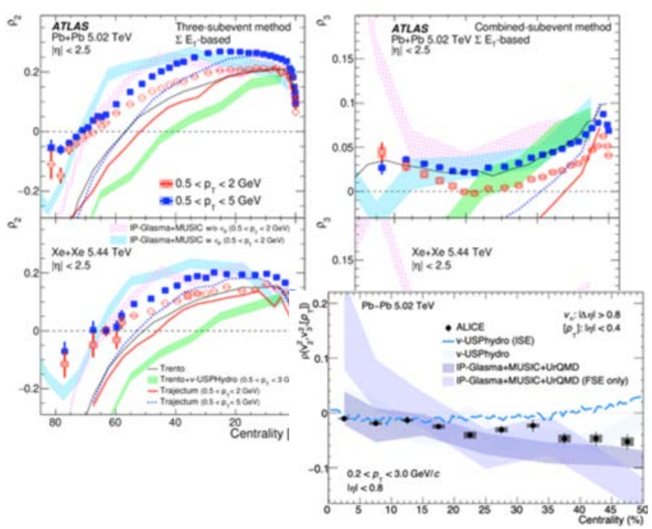

p_T fluctuations $p(p_T)$

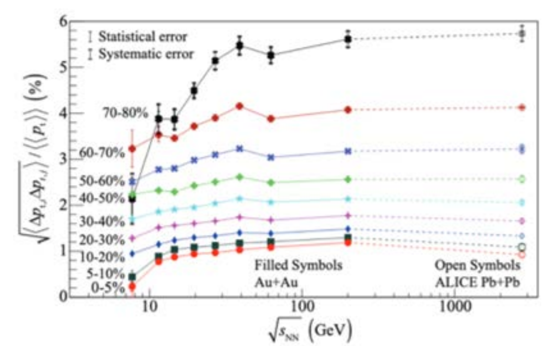

Challenges in HI and role of nuclear structure

Approach: state-of-the-art 3D hydro model + Bayesian inferences based on flow & other data. Challenge: simultaneously constrain two unknowns: <u>initial condition</u> and <u>QGP properties</u>. Status: QGP shear/bulk viscosity extraction limited by large uncertainties from initial condition

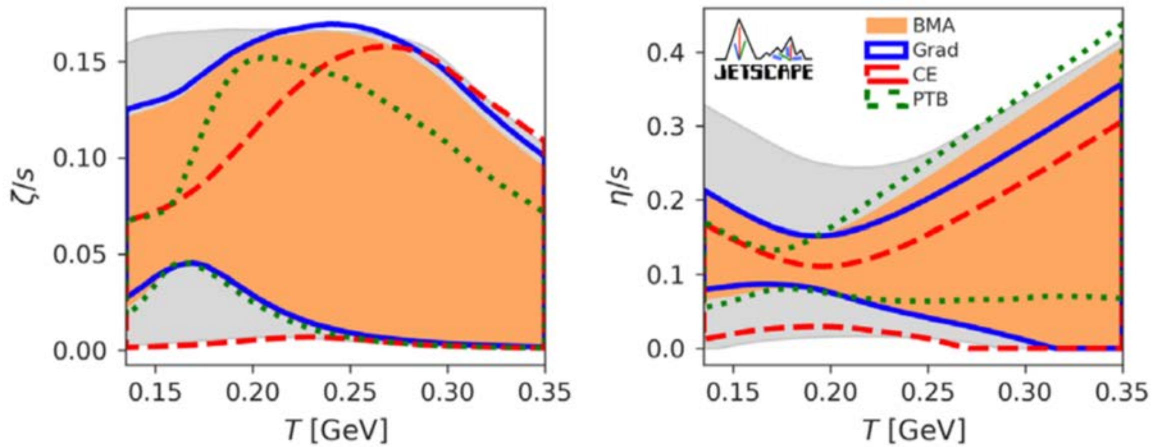

temperature dependence of viscosity

Strategy: constrain initial condition "independently" with nuclear structure input

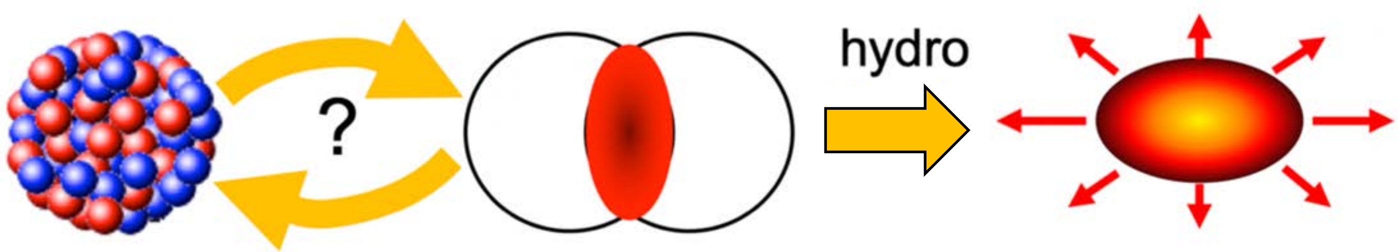

Constraints from nuclear structure ⇒ **Initial condition** ⇐ Constraints from Heavy ion observables

How deformation influence HI initial condition

Body-Body $\qquad \mathcal{E}_2 = \epsilon_2 e^{i2\Phi} \propto \left\langle \boldsymbol{r}_\perp^2 e^{i2\phi} \right\rangle \qquad$ Tip-Tip

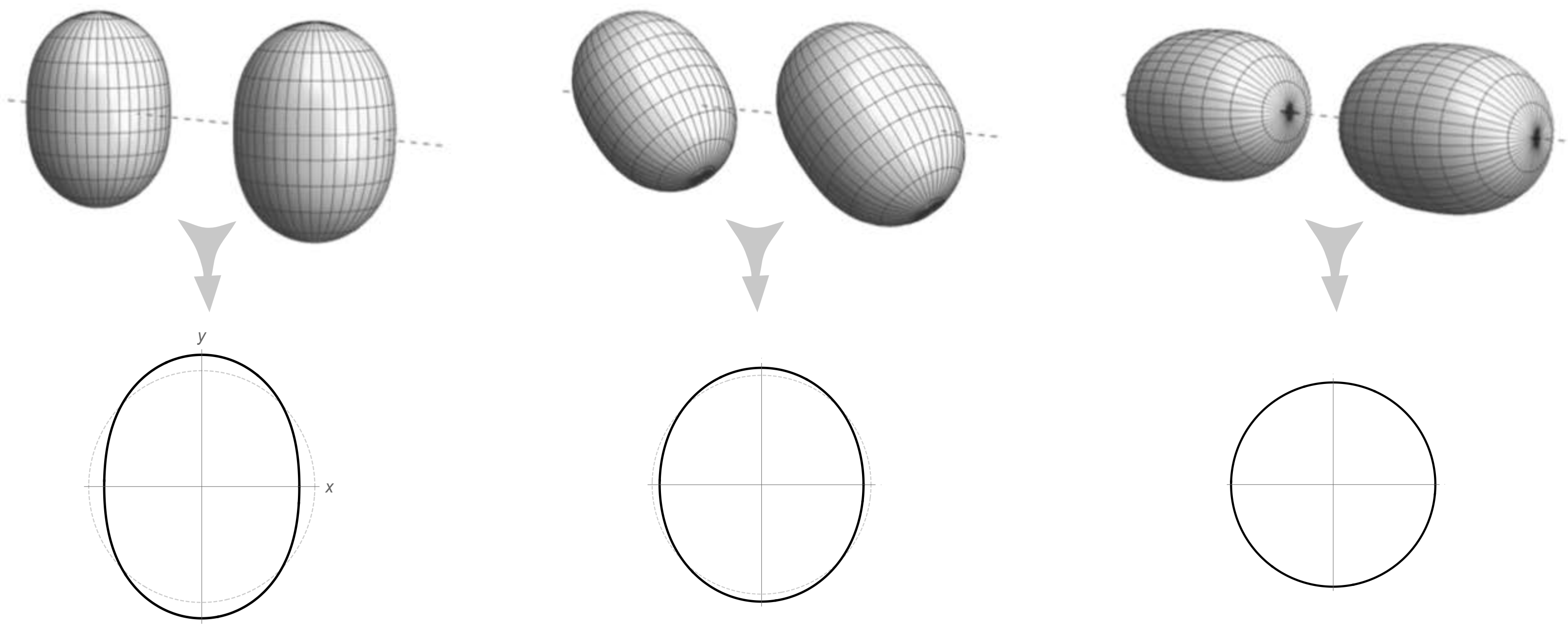

$\varepsilon_2 \sim 0.95\beta_2 \qquad \varepsilon_2 \sim 0.48\beta_2 \qquad \varepsilon_2 \sim 0$

$$\epsilon_2 = \underbrace{\epsilon_0}_{\text{undeformed}} + \underbrace{\boldsymbol{p}(\Omega_1, \Omega_2)}_{\text{phase factor}} \beta_2 + \mathcal{O}\left(\beta_2^2\right) \Longrightarrow \left\langle \epsilon_2^2 \right\rangle \approx \left\langle \epsilon_0^2 \right\rangle + 0.2\beta_2^2$$

$$\left\langle v_n^2 \right\rangle \propto \left\langle \epsilon_n^2 \right\rangle$$

Shape depends on Euler angle Ω=φθψ

Expected structure dependencies

arXiv:2106.08768

$$\langle v_n^2 \rangle \propto \langle \epsilon_n^2 \rangle \qquad \mathcal{E}_n = \epsilon_n e^{in\Phi} \propto \langle \boldsymbol{r}^2 Y_{n,n} \rangle$$

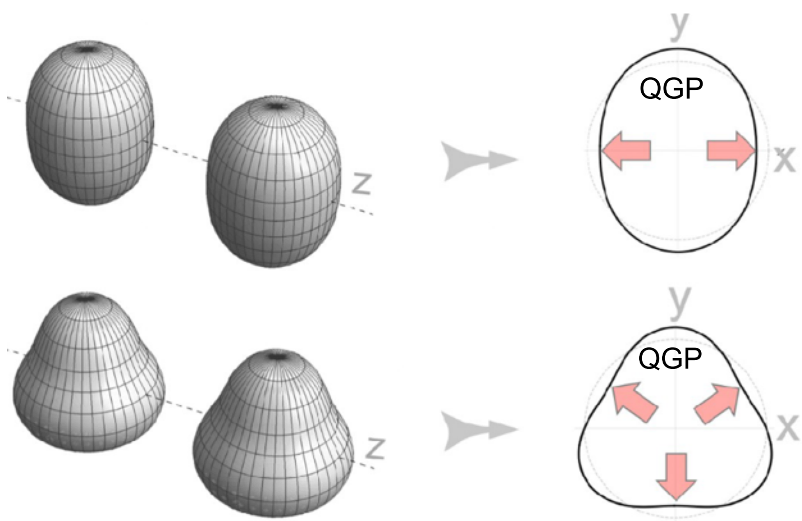

$$\langle v_2^2 \rangle \approx a_2 + b_2 \beta_2^2 + c_3 \beta_3^2$$

$$\frac{\delta[p_T]}{[p_T]} \propto -\frac{\delta R_\perp}{R_\perp} \qquad R_\perp^2 \propto \langle \boldsymbol{r}^2 Y_{2,0} \rangle$$

$$\left\langle (\delta p_{\mathrm{T}} / p_{\mathrm{T}})^2 \right\rangle \approx a_0 + b_0 \beta_2^2 + c_0 \beta_3^2$$

$$\langle v_3^2 \rangle \approx a_3 + b_3 \beta_3^2$$

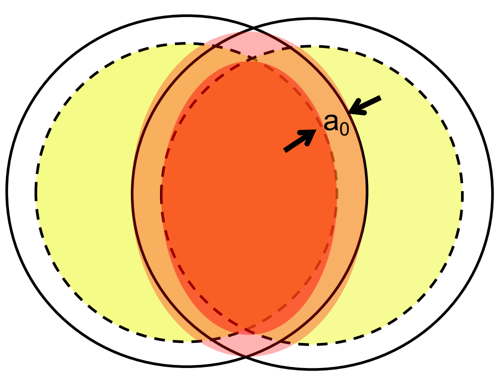

The shape and size the overlap, therefore v_2 and p_T, also depend on diffuseness a_0 and radius R_0

At fixed N_{part} $a_0 \searrow \Rightarrow v_2 \nearrow \quad p_T \nearrow$

$R_0 \searrow \Rightarrow p_T \nearrow$

Why β_3 influence ε_2?

$$\langle v_2^2 \rangle \approx a_2 + b_2\beta_2^2 + c_3\beta_3^2$$

Different from ε_2 and ε_3 anti-correlation observed for fluctuations

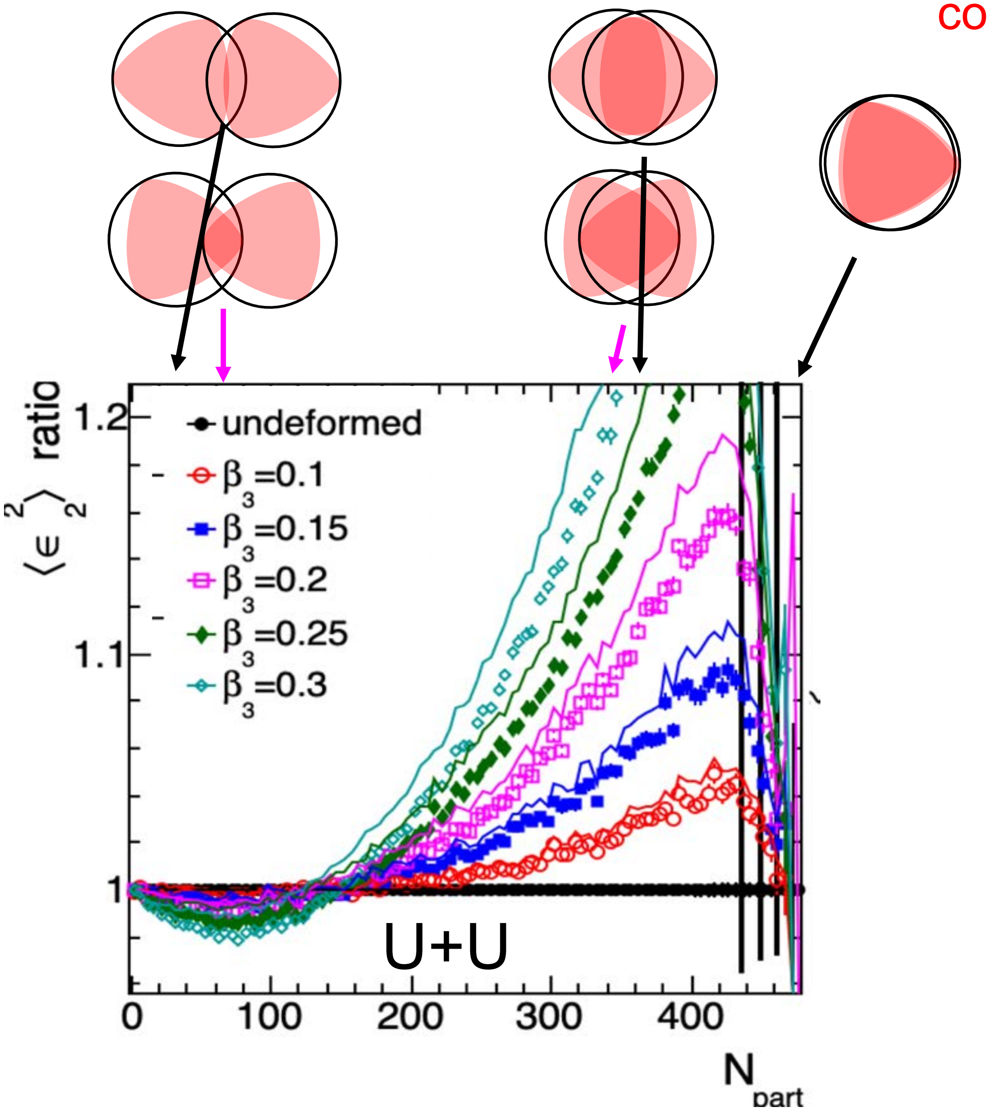

arXiv:2106.08768

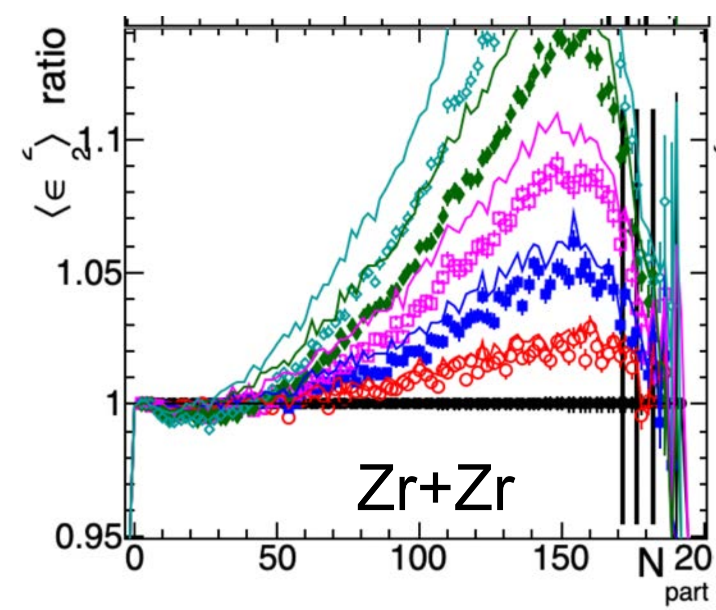

Low-energy vs high-energy HI method

- Shape from B(En), radial profile from e+A or ion-A scattering

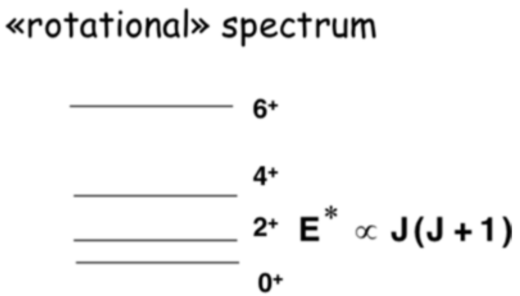

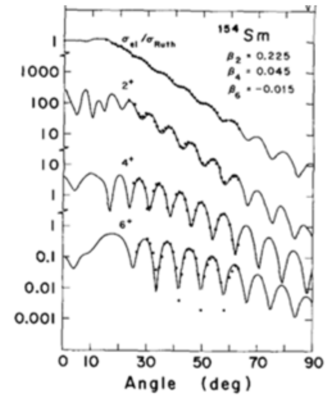

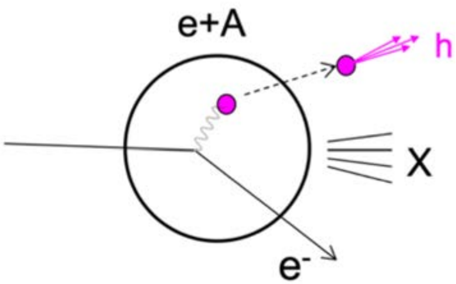

- Shape frozen in crossing time (<10^{-24}s), probe entire mass distribution via multi-point correlations.

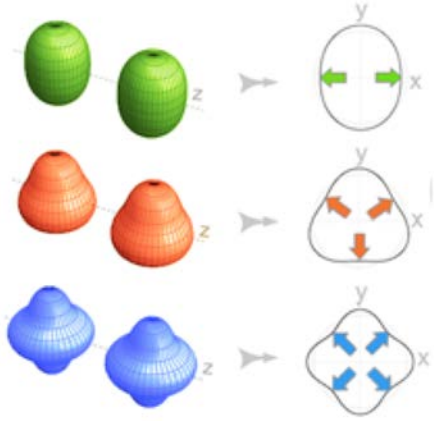

Collective flow response to nuclear structure

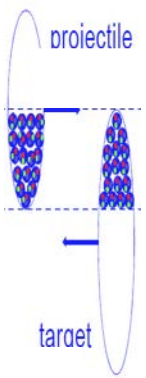

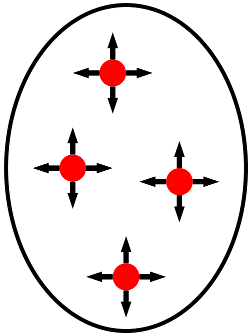

$$S(\mathbf{s}_1,\mathbf{s}_2) \equiv \langle \delta\rho(\mathbf{s}_1)\delta\rho(\mathbf{s}_2)\rangle = \langle \rho(\mathbf{s}_1)\rho(\mathbf{s}_2)\rangle - \langle \rho(\mathbf{s}_1)\rangle\langle \rho(\mathbf{s}_2)\rangle.$$

High-order fluctuations

- In principle, can measure any moments of p(1/R, ε_2, ε_3…)
  - Mean $\langle d_\perp \rangle$ $\quad\Rightarrow\quad$ $\langle p_T \rangle$
  - Variances: $\langle \varepsilon_n^2 \rangle, \left\langle (\delta d_\perp / d_\perp)^2 \right\rangle$ $\quad d_\perp \equiv 1/R_\perp$ $\quad\Rightarrow\quad$ $\langle v_n^2 \rangle, \left\langle (\delta p_T / p_T)^2 \right\rangle$
  - Skewness $\langle \varepsilon_n^2 \delta d_\perp / d_\perp \rangle, \left\langle (\delta d_\perp / d_\perp)^3 \right\rangle$ $\quad\Rightarrow\quad$ $\langle v_n^2 \delta p_T / p_T \rangle, \left\langle (\delta p_T / p_T)^3 \right\rangle$
  - Kurtosis $\langle \varepsilon_n^4 \rangle - 2\langle \varepsilon_n^2 \rangle^2, \left\langle (\delta d_\perp / d_\perp)^4 \right\rangle - 3\left\langle (\delta d_\perp / d_\perp)^2 \right\rangle^2$ $\quad\Rightarrow\quad$ $\langle v_n^4 \rangle - 2\langle v_n^2 \rangle^2, \left\langle (\delta p_T / p_T)^4 \right\rangle - 3\left\langle (\delta p_T / p_T)^2 \right\rangle^2$

    …

- All with rather simple connection to deformation, for example:
  - Variances

$$\langle \varepsilon_2^2 \rangle \sim a_2 + b_2 \beta_2^2 + b_{2,3} \beta_3^2$$
$$\langle \varepsilon_3^2 \rangle \sim a_3 + b_3 \beta_3^2 + b_{3,2} \beta_2^2 + b_{3,4} \beta_4^2$$
$$\langle \varepsilon_4^2 \rangle \sim a_4 + b_4 \beta_4^2 + b_{4,2} \beta_2^2$$
$$\langle (\delta d_\perp / d_\perp)^2 \rangle \sim a_0 + b_0 \beta_2^2 + b_{0,3} \beta_3^2$$

  - Skewness

$$\left\langle \varepsilon_2^2 \delta d_\perp / d_\perp \right\rangle \sim a_1 - b_1 \cos(3\gamma) \beta_2^3$$
$$\left\langle (\delta d_\perp / d_\perp)^3 \right\rangle \sim a_2 + b_2 \cos(3\gamma) \beta_2^3$$

  - Kurtosis

$$\left\langle \varepsilon_2^4 \right\rangle - 2\left\langle \varepsilon_2^2 \right\rangle^2 \sim a_3 - b_3 \beta_2^4$$
$$\left\langle (\delta d_\perp / d_\perp)^4 \right\rangle - 3\left\langle (\delta d_\perp / d_\perp)^2 \right\rangle^2 \sim a_4 - b_4 \beta_2^4$$

Isobar collisions at RHIC: a precision tool

Fuqiang Wang's talk

	Z	N	mass
96Ru	44	52	95.907598(8)
96Zr	40	56	95.908273(3)

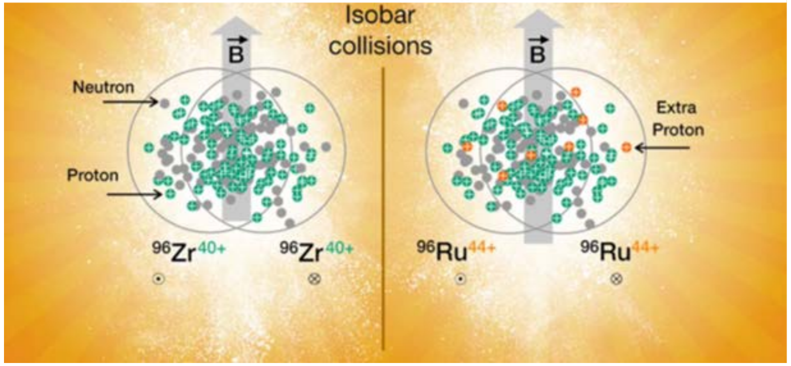

arXiv:2109.00131

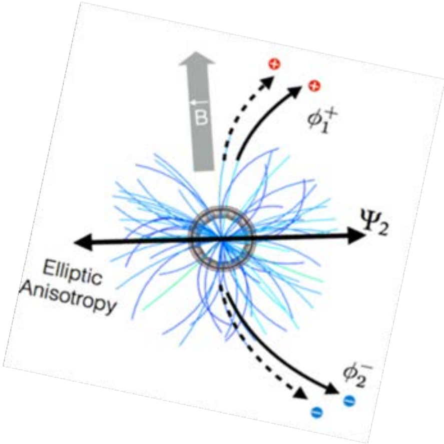

Voloshin, hep-ph/0406311

- Designed to search for the chiral magnetic effect: strong P & CP violation of QCD in the presence of EM field. Turns out the CME signal is small, and isobar-differences are dominated by the nuclear structure differences.

- <0.4% precision is achieved in ratio of many observables between ^{96}Ru+ ^{96}Ru and ^{96}Zr+^{96}Zr systems→ precision imaging tool

-

Isobar collisions at RHIC: a precision tool

- A key question for any HI observable O:

$$\boxed{\frac{O_{^{96}\mathrm{Ru}+^{96}\mathrm{Ru}}}{O_{^{96}\mathrm{Zr}+^{96}\mathrm{Zr}}} \stackrel{?}{=} 1}$$

Deviation from 1 must has origin in the nuclear structure, which impacts the initial state and then survives to the final state.

- Expectation

$$\rho(r,\theta,\phi) \propto \frac{1}{1+e^{[r-R_0(1+\beta_2 Y_2^0(\theta,\phi)+\beta_3 Y_3^0(\theta,\phi))]/a_0}}$$

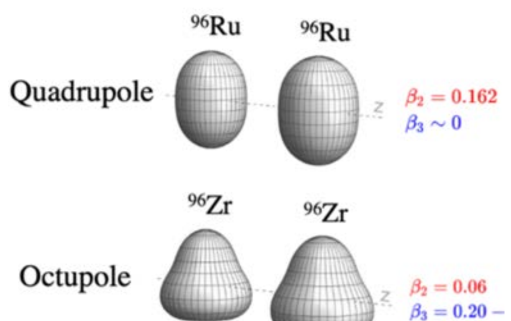

J. Jia, aXiv:2106.08768

2109.00131

$$\mathcal{O} \approx b_0 + b_1\beta_2^2 + b_2\beta_3^2 + b_3(R_0 - R_{0,\mathrm{ref}}) + b_4(a - a_{\mathrm{ref}})$$

$$\boxed{R_{\mathcal{O}} \equiv \frac{\mathcal{O}_{\mathrm{Ru}}}{\mathcal{O}_{\mathrm{Zr}}} \approx 1 + c_1\Delta\beta_2^2 + c_2\Delta\beta_3^2 + c_3\Delta R_0 + c_4\Delta a}$$

Only probes isobar differences

Species	β_2	β_3	a_0	R_0
Ru	0.162	0	0.46 fm	5.09 fm
Zr	0.06	0.20	0.52 fm	5.02 fm
difference	$\Delta\beta_2^2$	$\Delta\beta_3^2$	Δa_0	ΔR_0
	0.0226	-0.04	-0.06 fm	0.07 fm

Relate to neutron skin: $\Delta r_{\mathrm{np}} = \langle r_n \rangle^{1/2} - \langle r_p \rangle^{1/2}$

$$\Delta r_{np,\mathrm{Ru}} - \Delta r_{np,\mathrm{Zr}} \propto \underbrace{(R_0\Delta R_0 - \overbrace{R_{0p}\Delta R_{0p}) + 7/3\pi^2(a\Delta a}^{\text{charge}}}_{\text{mass}} - a_p\Delta a_p)$$

Structure influences everywhere

$$R_{\mathcal{O}} \equiv \frac{\mathcal{O}_{\mathrm{Ru}}}{\mathcal{O}_{\mathrm{Zr}}}$$

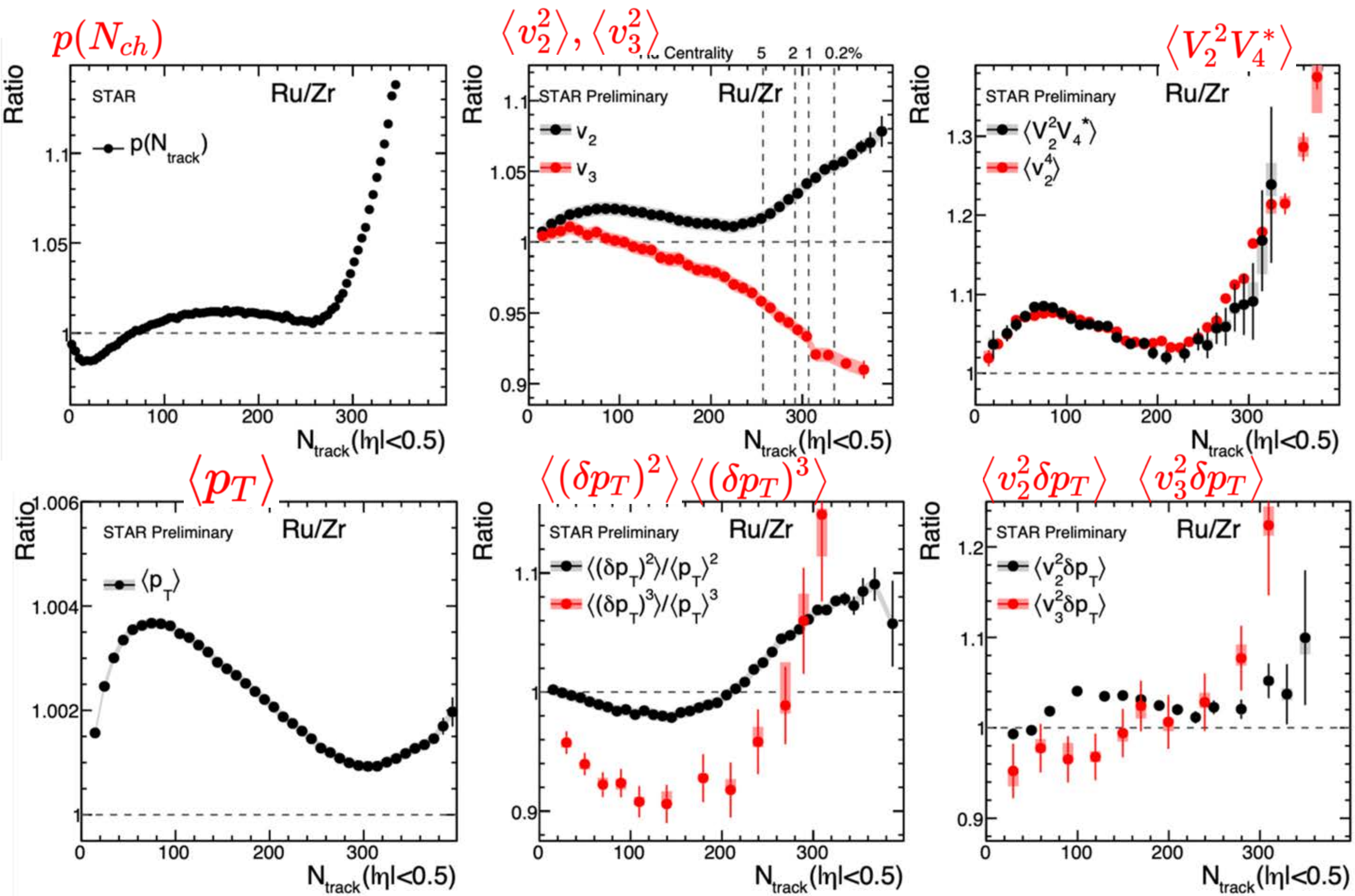

-

Nuclear structure via v_2-ratio and v_3-ratio

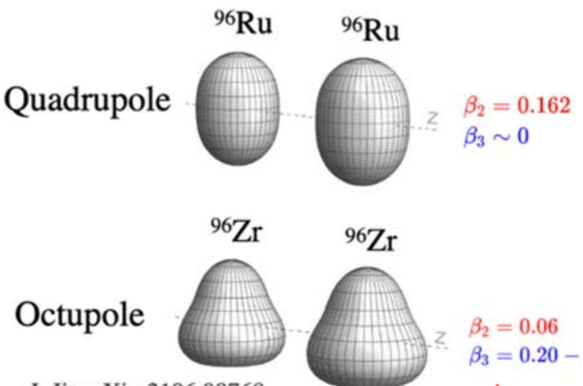

J. Jia, aXiv:2106.08768

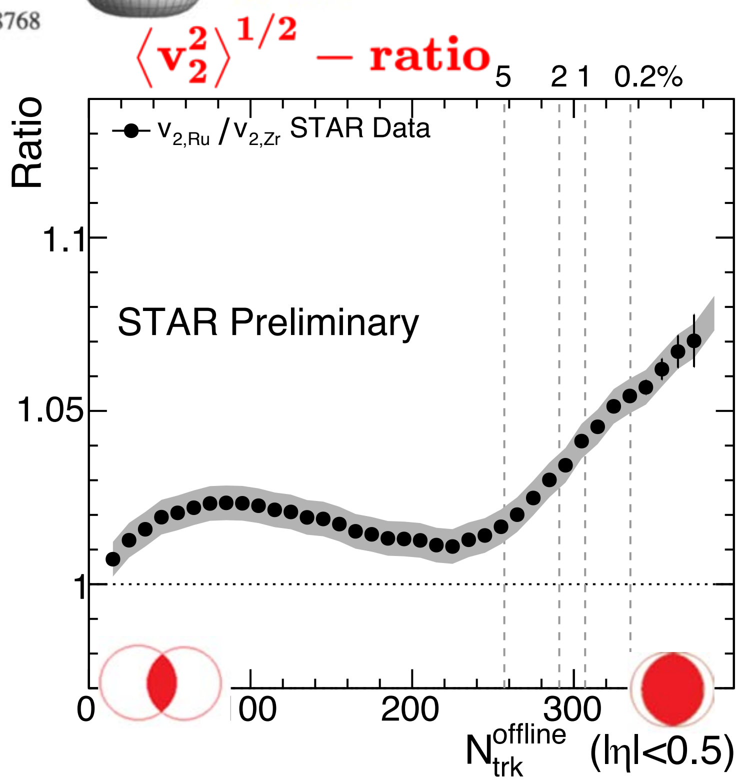

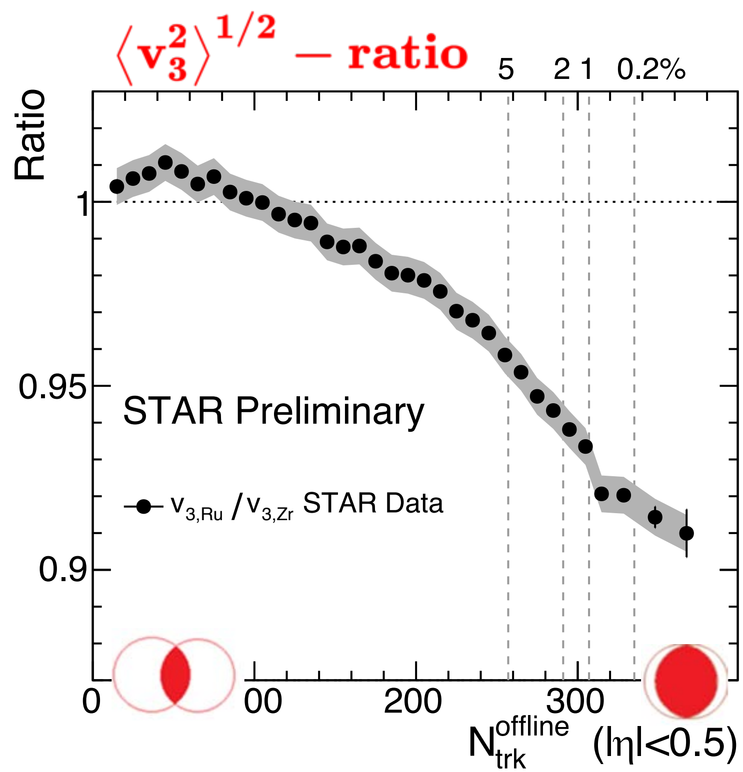

Nuclear structure via v_2-ratio and v_3-ratio

- β_{2Ru}~0.16 increase v_2, no influence on v_3 ratio

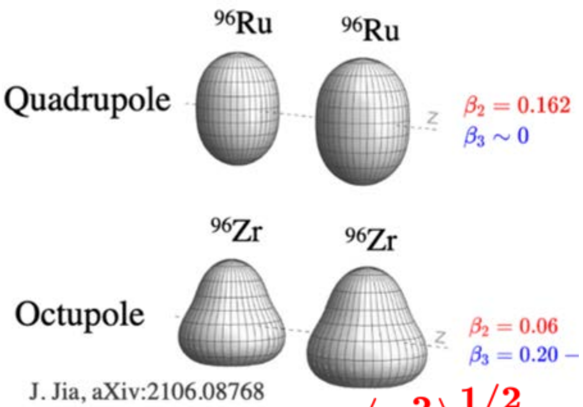

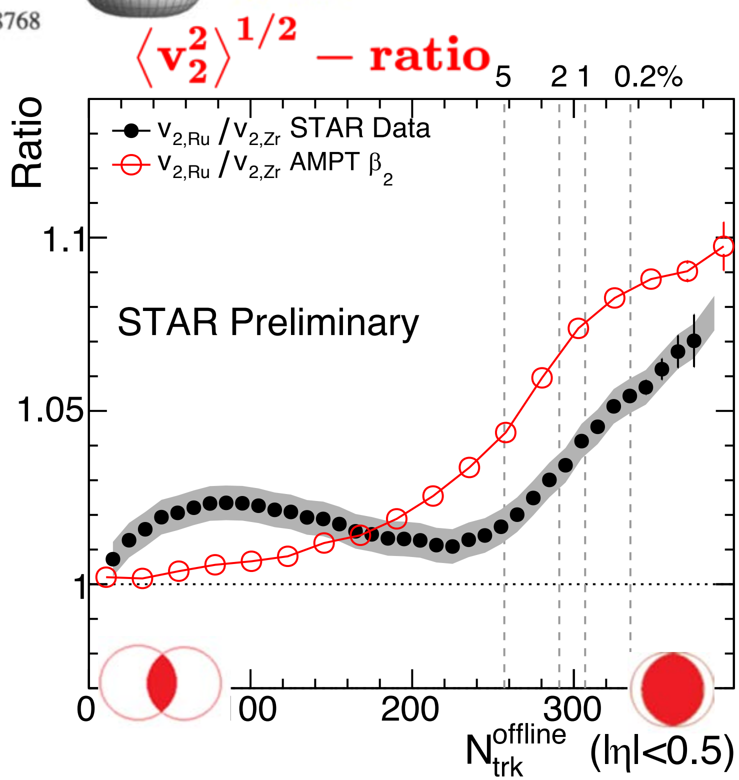

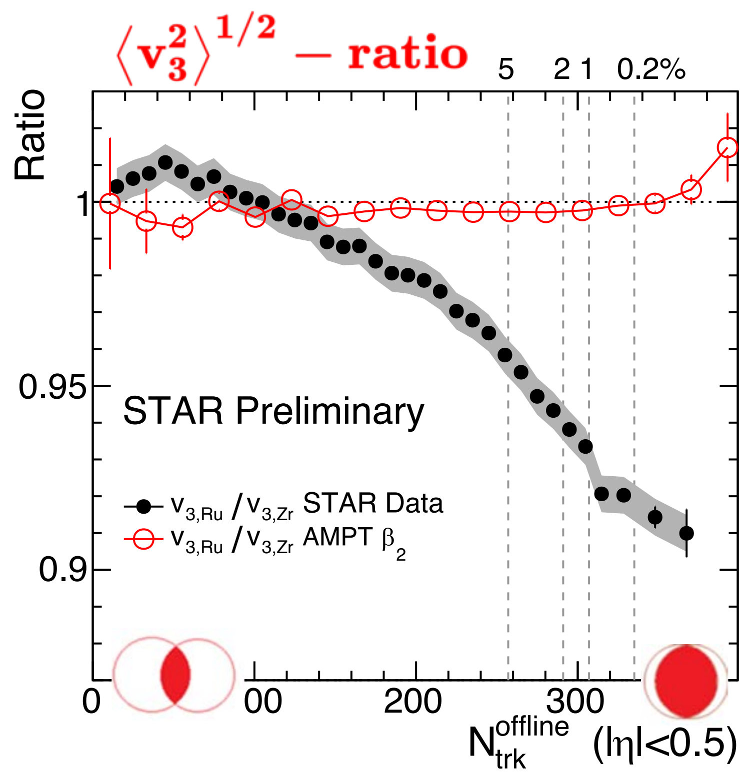

Nuclear structure via v_2-ratio and v_3-ratio

- β_{2Ru}~0.16 increase v_2, no influence on v_3 ratio
- β_{3Zr}~0.2 decrease v_2 in mid-central, decrease v_3 ratio

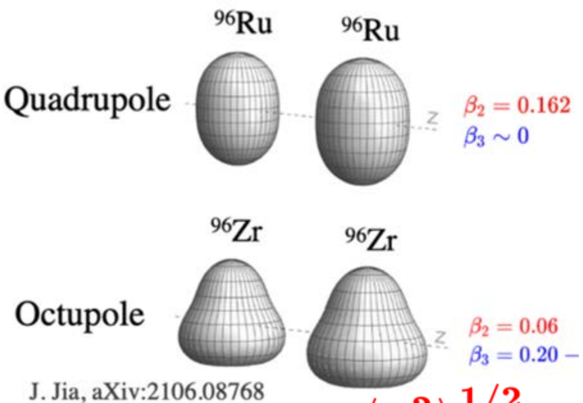

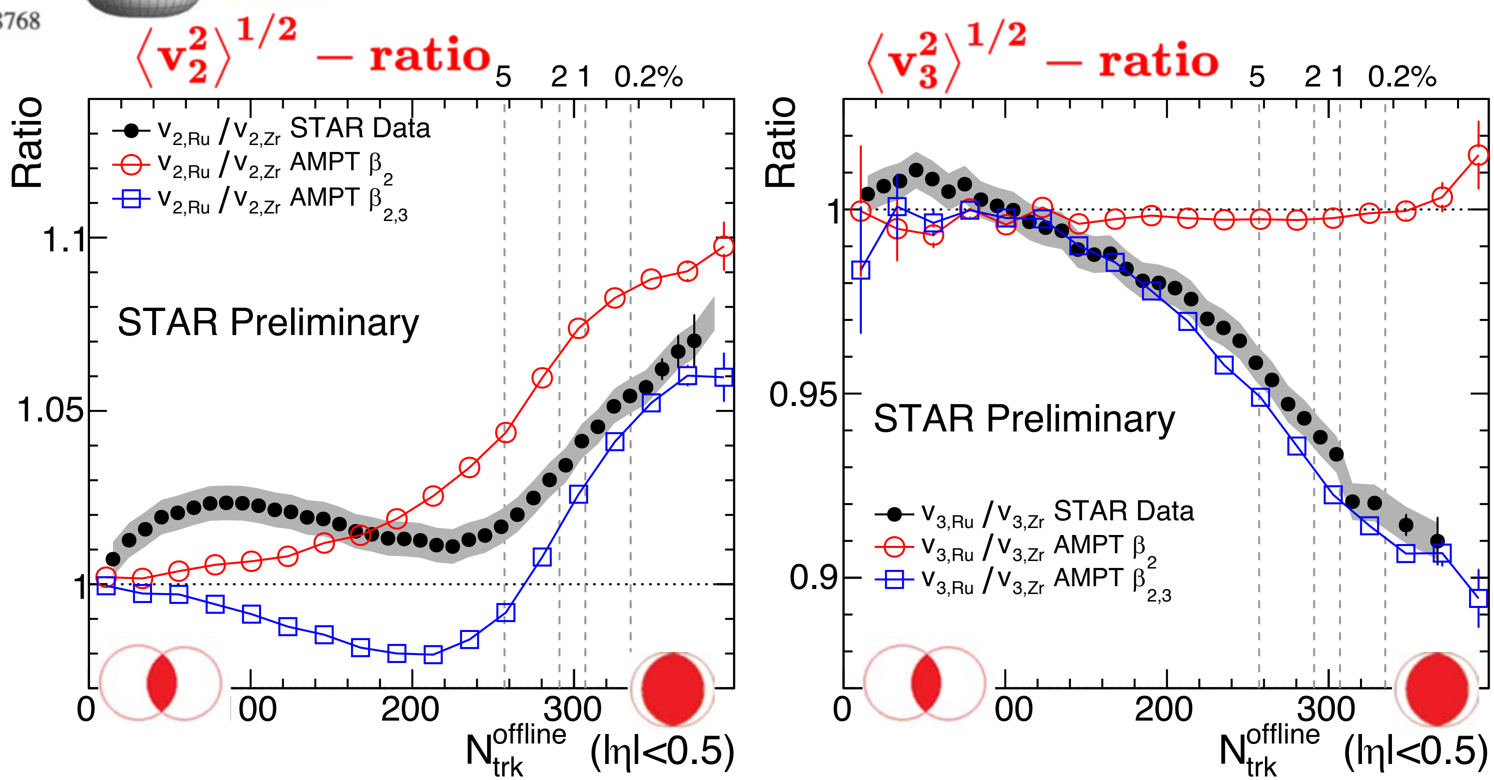

Nuclear structure via v_2-ratio and v_3-ratio

- β_{2Ru}~0.16 increase v_2, no influence on v_3 ratio
- β_{3Zr}~0.2 decrease v_2 in mid-central, decrease v_3 ratio
- Δa_0= -0.06fm increase v_2 mid-central, small influ. on v_3.

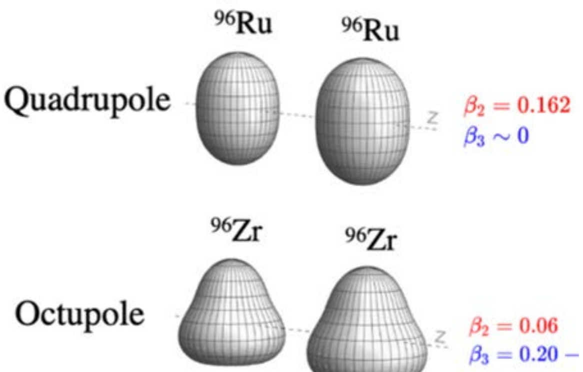

J. Jia, aXiv:2106.08768

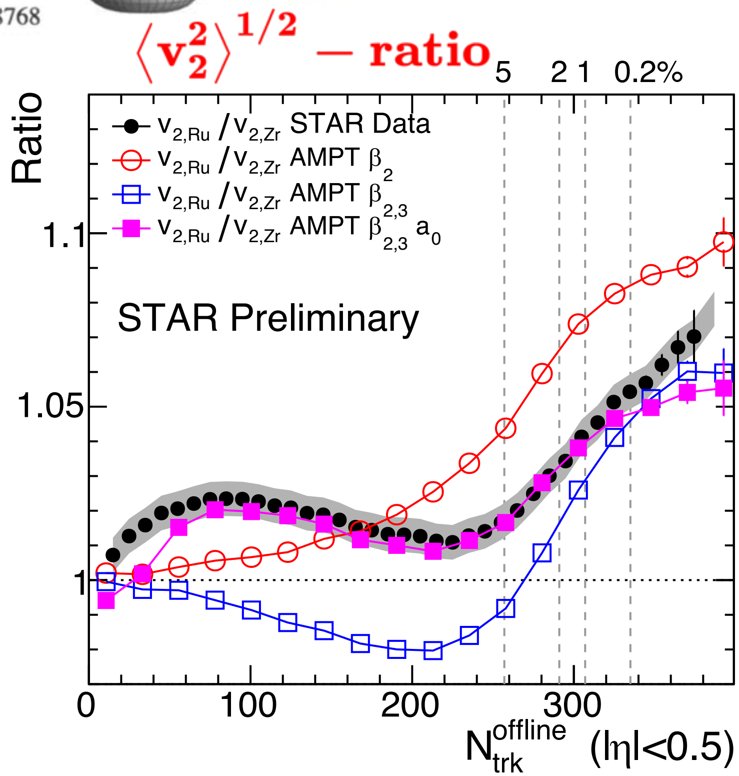

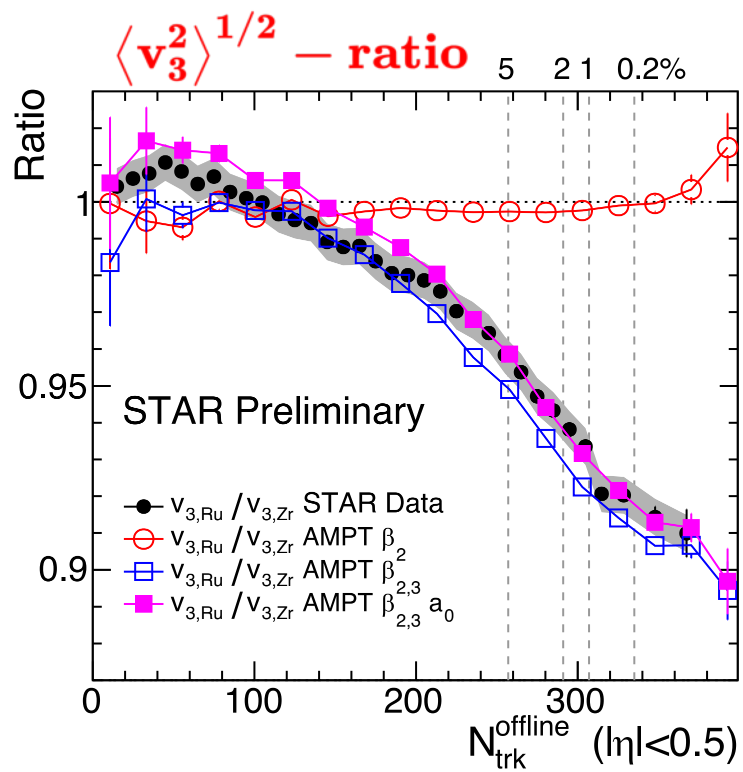

Nuclear structure via v_2-ratio and v_3-ratio

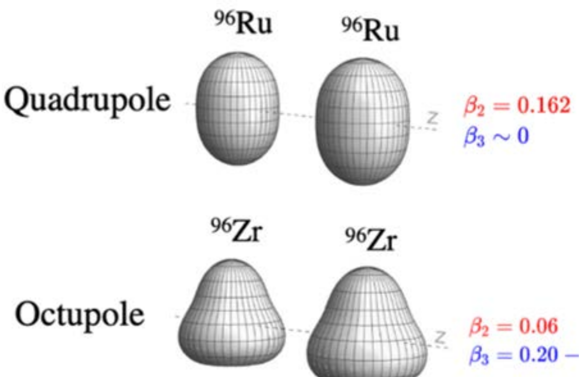

J. Jia, aXiv:2106.08768

- β_{2Ru}~0.16 increase v_2, no influence on v_3 ratio
- β_{3Zr}~0.2 decrease v_2 in mid-central, decrease v_3 ratio
- Δa_0= -0.06fm increase v_2 mid-central, small influ. on v_3.
- Radius ΔR_0=0.07fm only slightly affects v_2 and v_3 ratio.

$$R_{\mathcal{O}} \equiv \frac{\mathcal{O}_{\rm Ru}}{\mathcal{O}_{\rm Zr}} \approx 1 + c_1\Delta\beta_2^2 + c_2\Delta\beta_3^2 + c_3\Delta R_0 + c_4\Delta a$$

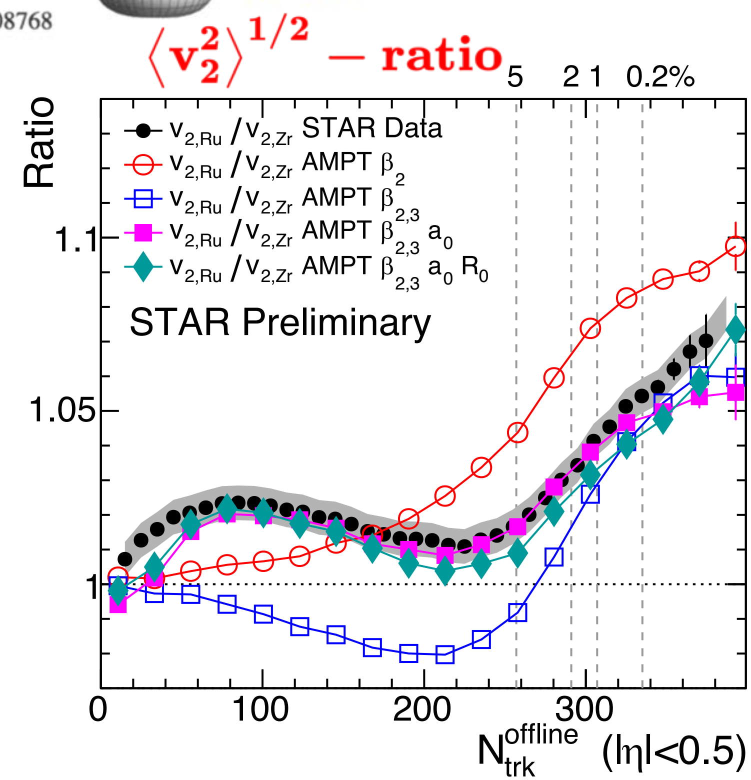

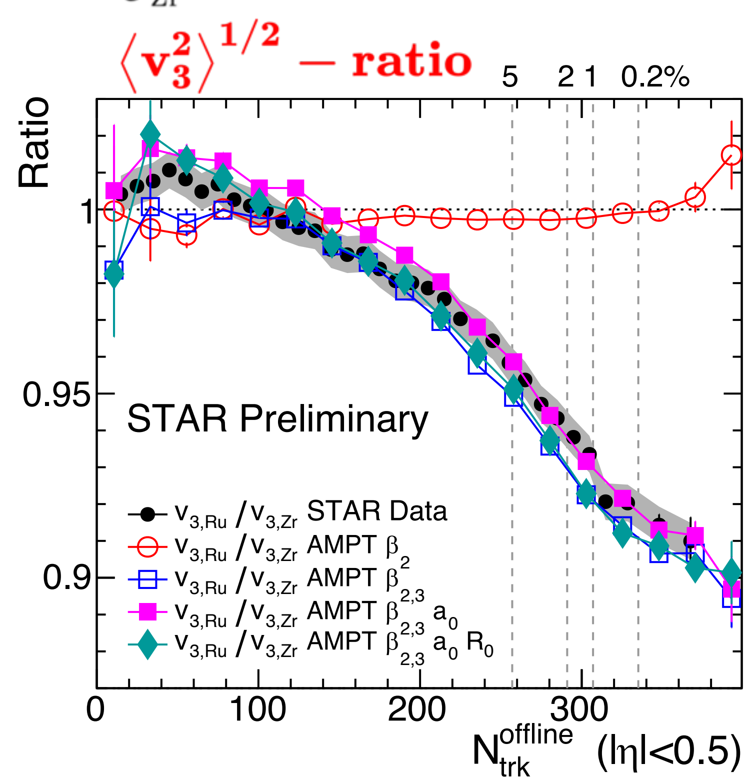

Simultaneously constrain these parameters using different N_{ch} regions

Nuclear structure via $p(N_{ch})$, $\langle p_T \rangle$-ratio

Earlier studies on this from H.Li, H.J Xu, PRL125, 222301 (2020) arXiv:2111.14812

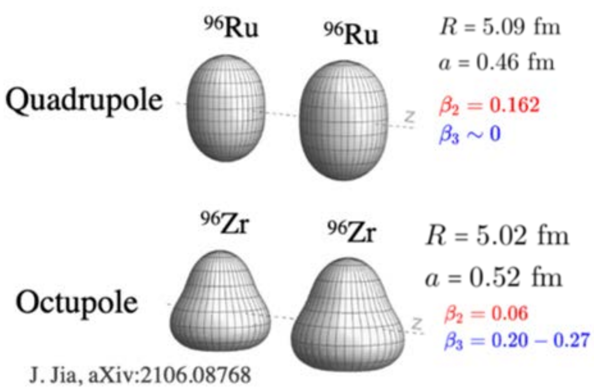

- For N_{ch} ratio:
  - β_{2Ru}~0.16 decrease ratio, increase after considering β_{3Zr}~0.2
  - The bump structure in non-central region from Δa_0 and ΔR_0
- For $\langle p_T \rangle$ ratio:
  - Strong influence from Δa_0 and ΔR_0

$$R_{\mathcal{O}} \equiv \frac{\mathcal{O}_{\rm Ru}}{\mathcal{O}_{\rm Zr}} \approx 1 + c_1 \Delta\beta_2^2 + c_2 \Delta\beta_3^2 + c_3 \Delta R_0 + c_4 \Delta a$$

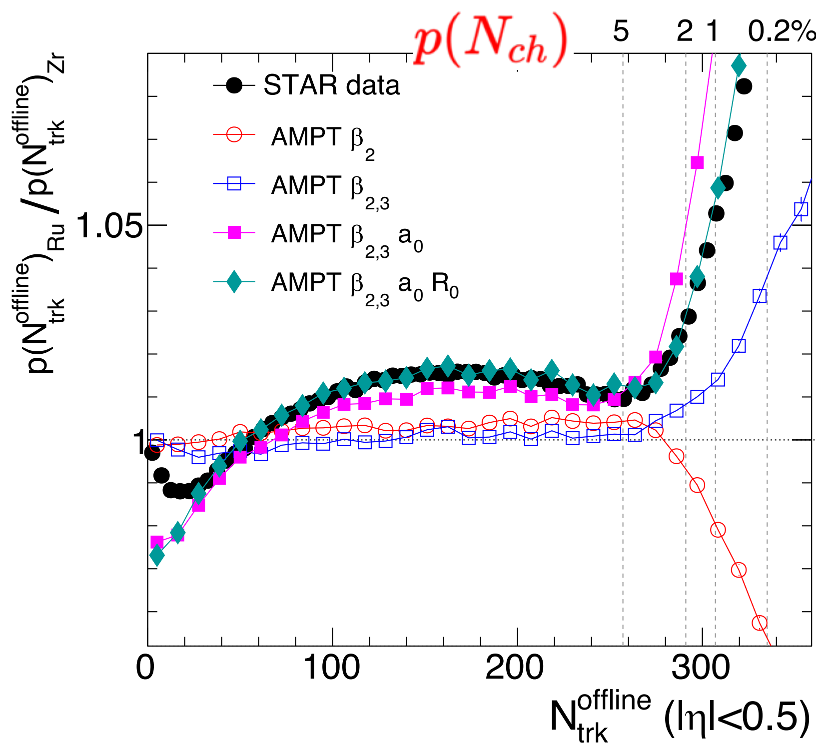

Δa_0 and ΔR_0 influences add up

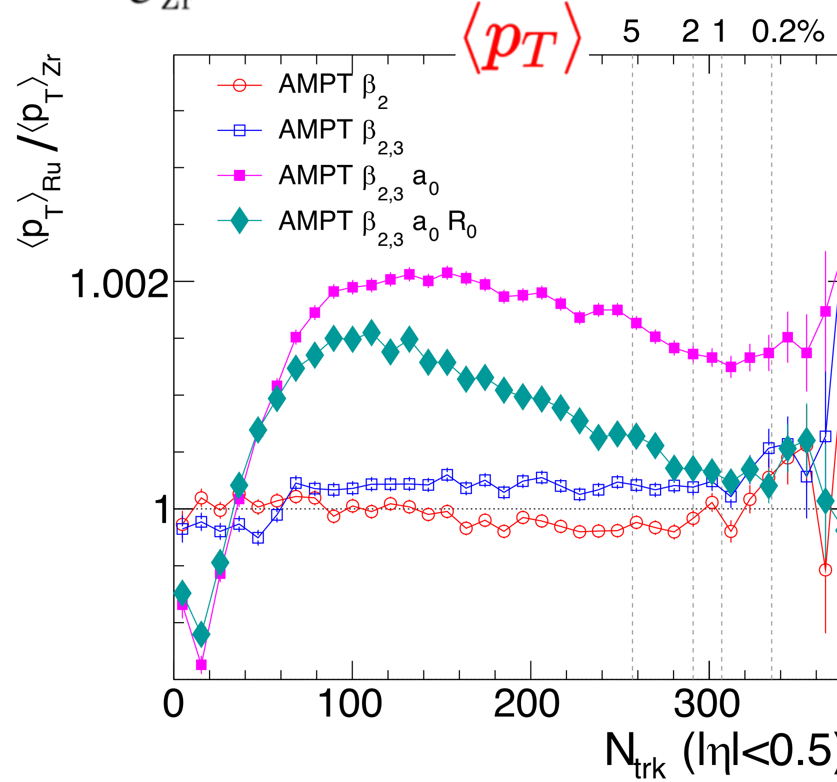

Δa_0 and ΔR_0 influences partially cancel

Isobar ratios not affected by final state

- Vary the shear viscosity via partonic cross-section
  - Flow signal change by 30-50%, the v_n ratio unchanged.

$$v_n = k_n \varepsilon_n$$

$$\frac{v_{n,\mathrm{Ru}}}{v_{n,\mathrm{Zr}}} \approx \frac{\varepsilon_{n,\mathrm{Ru}}}{\varepsilon_{n,\mathrm{Zr}}}$$

Confirmed in Trajectum

Robust probe of initial state!

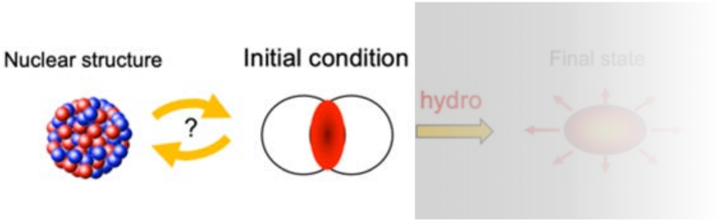

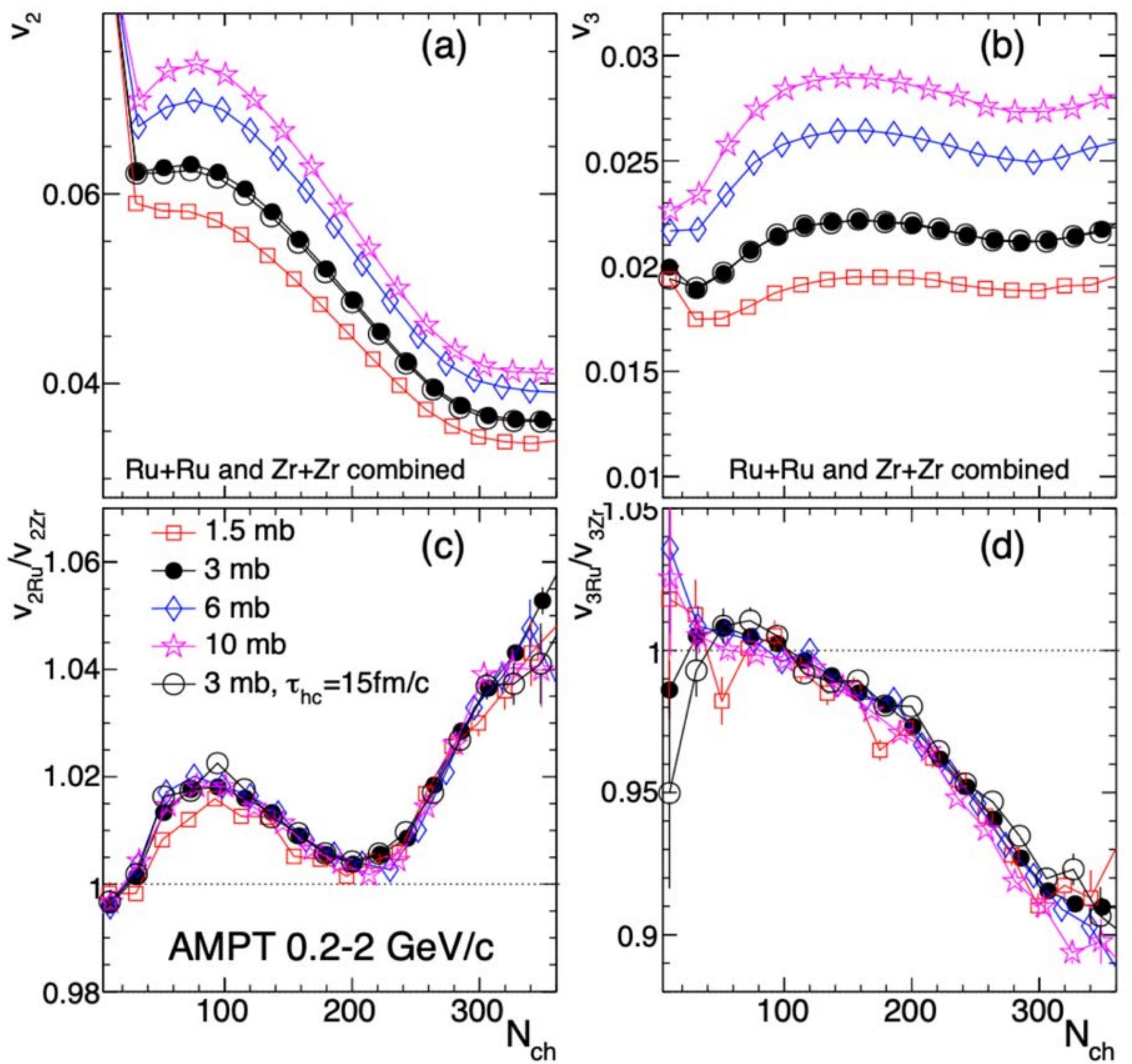

Isobar to constrain initial condition

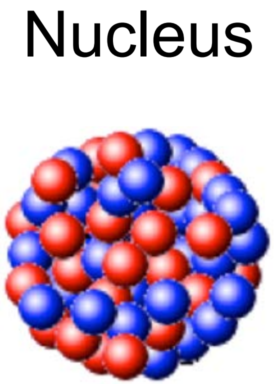

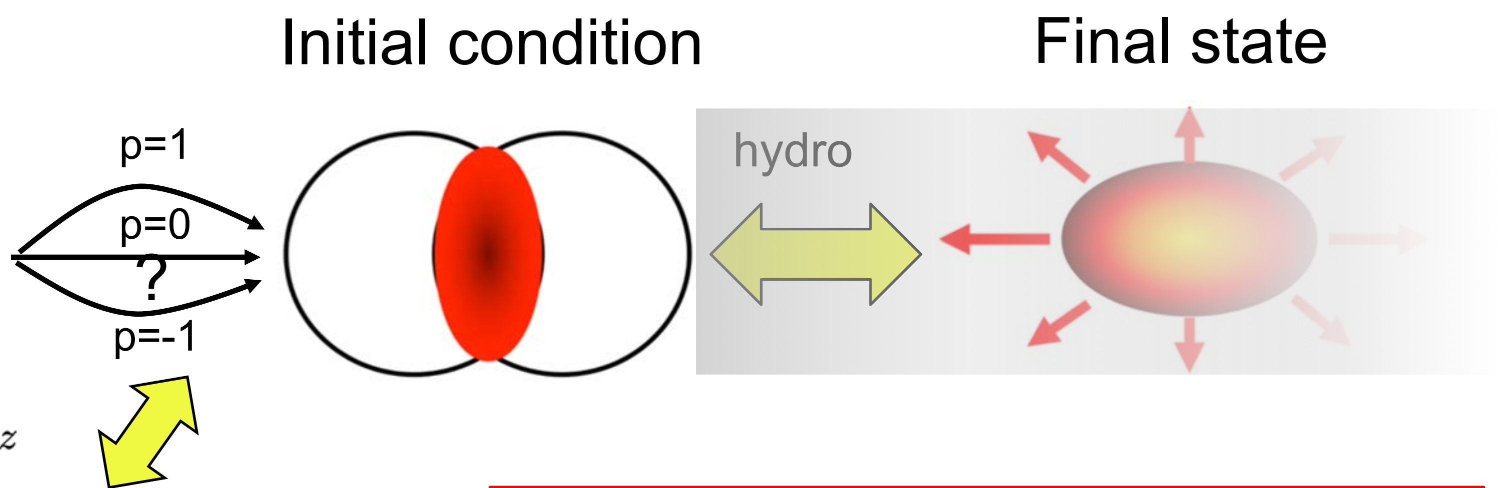

$$T_A(x,y) = \int \rho(x,y,z)dz$$

c_n relates nuclear structure and initial condition

See talk by A. Kirchner and F. Taghavi

$$\boxed{\frac{\mathcal{O}_{\mathrm{Ru}}}{\mathcal{O}_{\mathrm{Zr}}} \approx 1 + c_1\Delta\beta_2^2 + c_2\Delta\beta_3^2 + c_3\Delta R_0 + c_4\Delta a}$$

- Different ways of depositing energy $\quad T \propto \left(\frac{T_A^p + T_B^p}{2}\right)^{q/p}$

$$e(x,y) \sim \begin{cases} T_A + T_B & N_{\mathrm{part}} - \mathrm{scaling}, p = 1 \\ T_A T_B & N_{\mathrm{coll}} - \mathrm{scaling}, p = 0, q = 2 \\ \sqrt{T_A T_B} & \mathrm{Trento\ default}, p = 0 \\ \min\{T_A, T_B\} & \mathrm{KLN\ model}, p \sim -2/3 \\ T_A + T_B + \alpha T_A T_B & \mathrm{two\text{-}component\ model,} \\ & \mathrm{similar\ to\ quark\text{-}glauber\ model} \end{cases}$$

Use nuclear structure as extra lever-arm for initial condition

Exploiting the lever-arm from nuclear structure

Flow observable = k ⊗ initial condition (structure)

QGP response,
a smooth function of N+Z

Structure of colliding nuclei,
non-monotonic function of N and Z

QGP

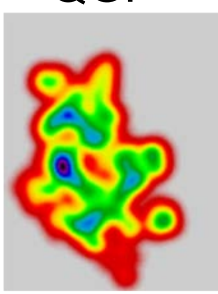

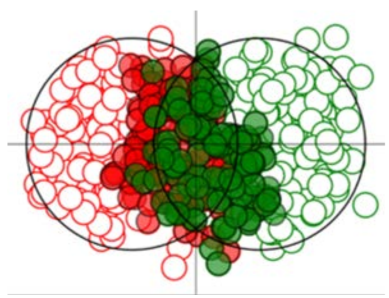

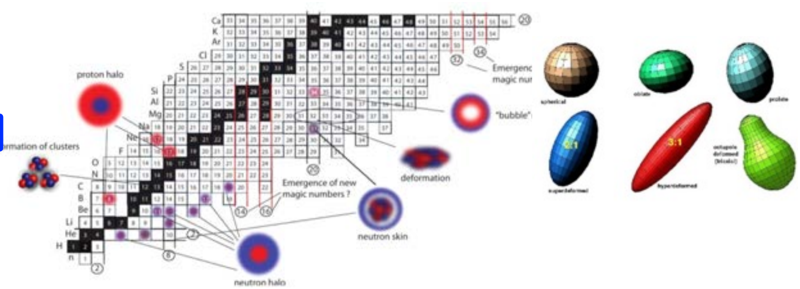

Example: shape evolution of $^{144-154}$Sm isotopic chain

Transition from nearly-spherical to well-deformed nuclei when size increase by less than 7%. Using HI to access the multi-nucleon correlations leading to such shape evolution, as well as dynamical β_3 and β_4 shape fluctuations (in addition to initial condition)

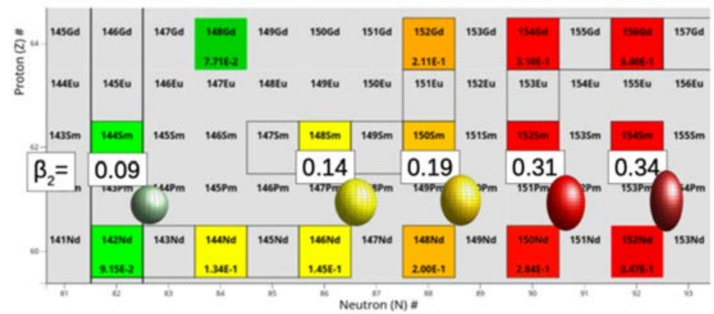

In central collisions

$$\left\langle \epsilon_2^2 \right\rangle = a' + b'\beta_2^2 \qquad a' = \langle \varepsilon_2^2 \rangle_{|\beta_2=0} \propto 1/A$$

$$\left\langle v_2^2 \right\rangle = a + b\beta_2^2 \qquad a = \langle v_2^2 \rangle_{|\beta_2=0} \propto 1/A$$

b', b are ~ independent of system

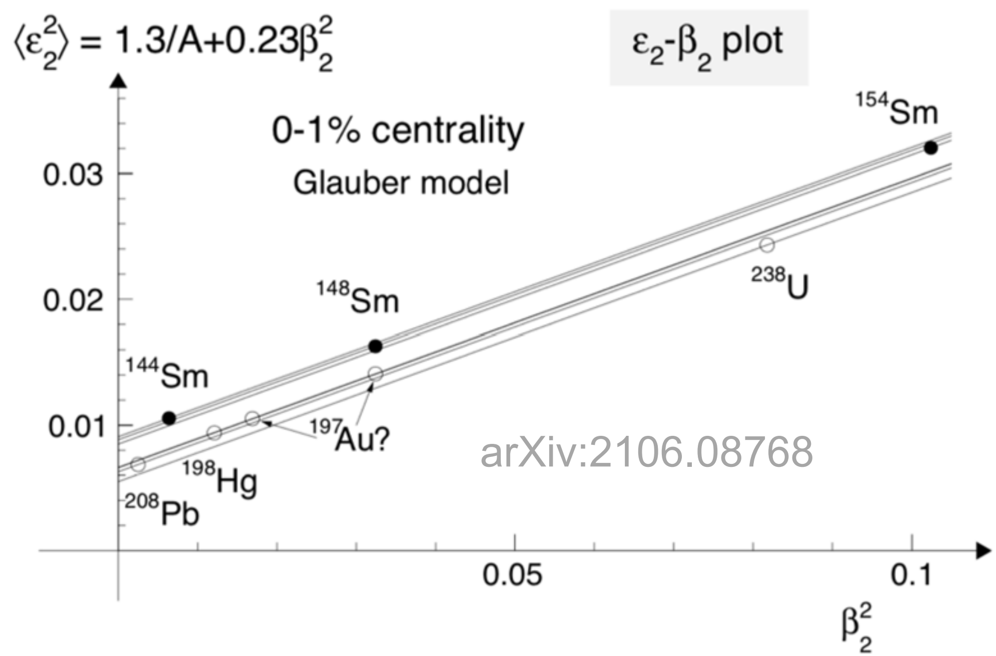

Systems with similar A falls on the same curve.

Fix a and b with two isobar systems with known β_2, then predict others.

Triaxility $R(\theta,\phi) = R_0\Big(1 + \beta_2[\cos\gamma Y_{2,0} + \sin\gamma Y_{2,2}]$

1910.04673, 2004.14463

Prolate

$\beta_2 = 0.25, \cos(3\gamma) = 1$

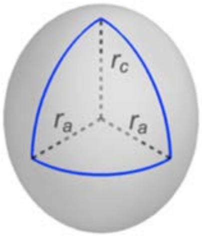

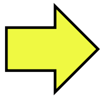

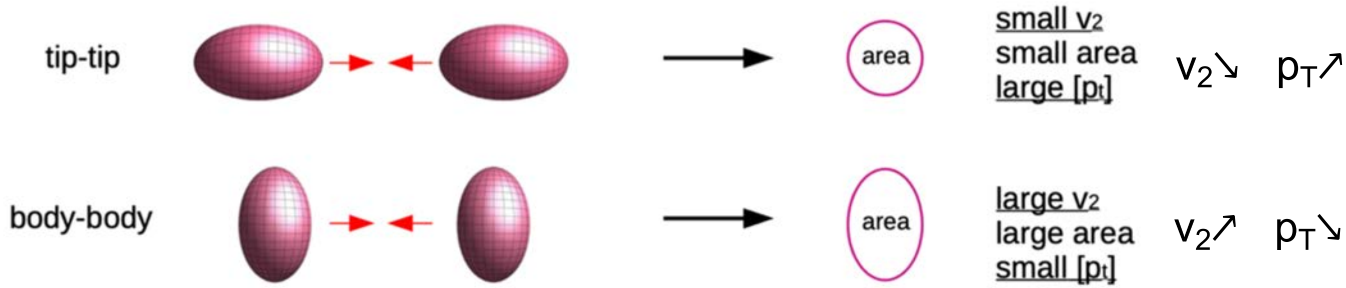

Need 3-point correlators to probe the 3 axes

$$\langle v_2^2 \delta p_T \rangle \sim -\beta_2^3 \cos(3\gamma) \qquad \langle (\delta p_T)^3 \rangle \sim \beta_2^3 \cos(3\gamma)$$

2109.00604

Triaxial

$\beta_2 = 0.25, \cos(3\gamma) = 0$

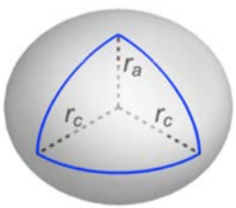

Oblate

$\beta_2 = 0.25, \cos(3\gamma) = -1$

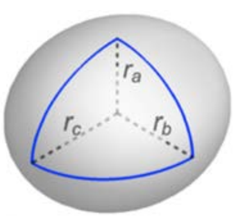

Triaxility

$$R(\theta,\phi) = R_0\left(1 + \beta_2[\cos\gamma Y_{2,0} + \sin\gamma Y_{2,2}]\right.$$

1910.04673, 2004.14463

Prolate

$\beta_2 = 0.25, \cos(3\gamma) = 1$

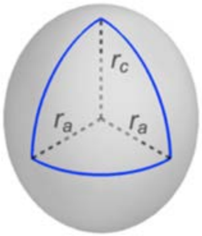

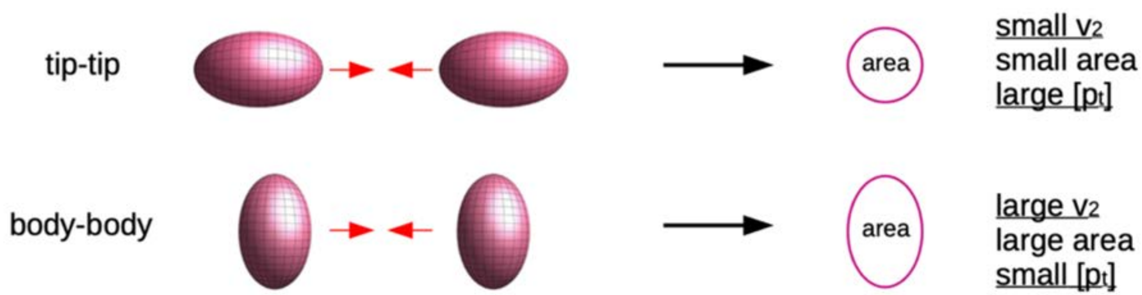

$v_2\searrow$ $p_T\nearrow$

$v_2\nearrow$ $p_T\searrow$

Need 3-point correlators to probe the 3 axes

$$\left\langle v_2^2\delta p_{\mathrm{T}}\right\rangle \sim -\beta_2^3\cos(3\gamma) \qquad \left\langle(\delta p_{\mathrm{T}})^3\right\rangle \sim \beta_2^3\cos(3\gamma)$$

2109.00604

Triaxial

$\beta_2 = 0.25, \cos(3\gamma) = 0$

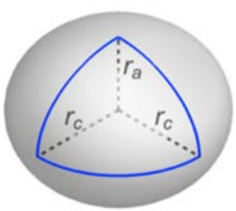

Oblate

$\beta_2 = 0.25, \cos(3\gamma) = -1$

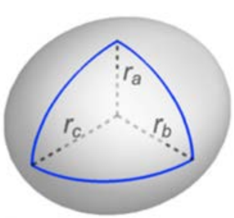

Compare U+U vs Au+Au: β_{2U} ~ 0.28, β_{2Au}~ 0.13:

v_2-[p_T] covariance

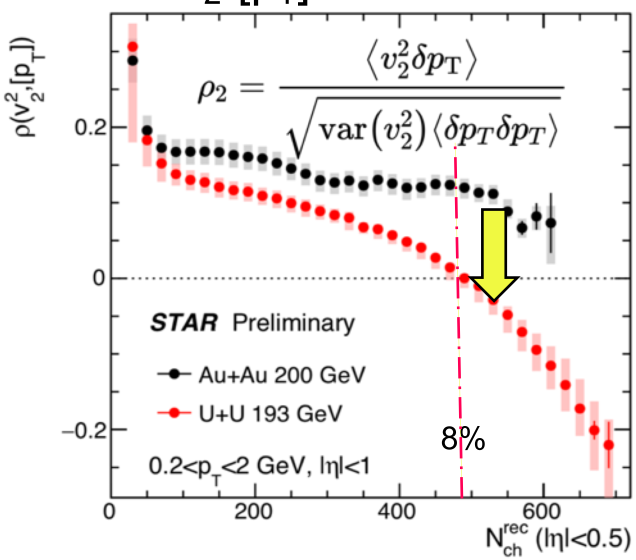

[p_T] skewness

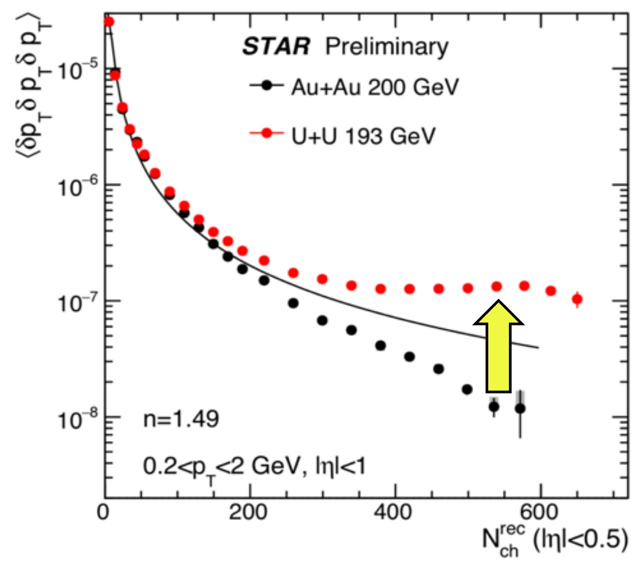

Influence of triaxiality: Glauber model

Skewness sensitive to γ

Described by

$$\left\langle \varepsilon_2^2 \frac{\delta d_\perp}{d_\perp} \right\rangle \propto \langle v_2^2 \delta p_{\mathrm{T}} \rangle \propto a + b\cos(3\gamma)\beta_2^3$$

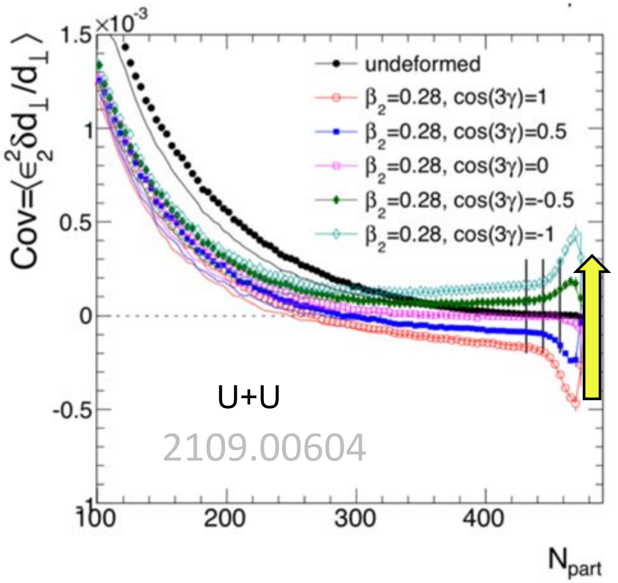

variances insensitive to γ

$$\langle \varepsilon_2^2 \rangle \propto \langle v_2^2 \rangle \propto a + b\beta_2^2$$

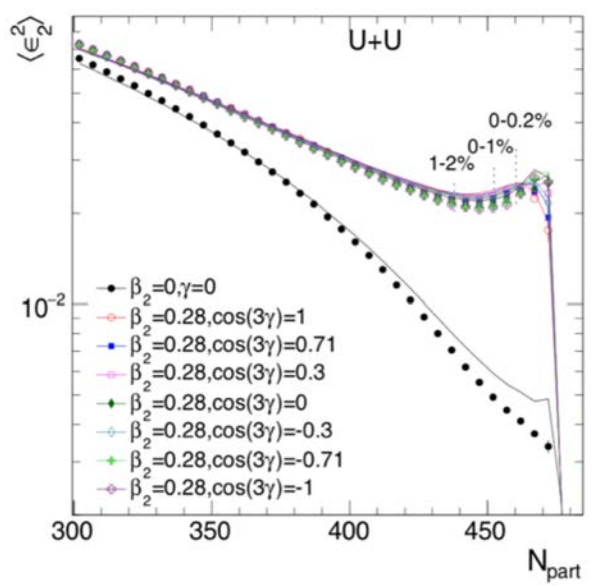

Use variance to constrain β_2, use skewness to constrain γ

(β_2,γ) diagram in heavy-ion collisions

The (β_2,γ) dependence in 0-1% U+U Glauber model can be approximated by:

$$d_\perp \propto 1/R_\perp$$

$$\langle\varepsilon_2^2\rangle \approx [0.02 + \beta_2^2] \times 0.235$$

$$\langle(\delta d_\perp/d_\perp)^2\rangle \approx [0.035 + \beta_2^2] \times 0.0093$$

$$\langle\varepsilon_2^2 \delta d_\perp/d_\perp\rangle \approx [0.0005 - (0.07 + 1.36\cos(3\gamma))\beta_2^3] \times 10^{-2}$$

$$\rho = \frac{\langle\varepsilon_2^2 \delta d_\perp\rangle}{\langle\varepsilon_2^2\rangle\sqrt{\langle(\delta d_\perp)^2\rangle}}$$

Map from (β_2,γ) plane to HI observables

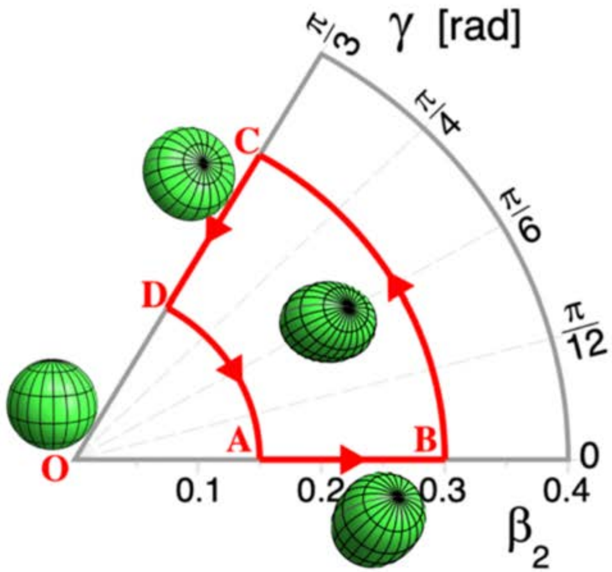

?

How about

$\langle v_2^2 \delta[p_T]\rangle$ vs. $\langle v_2^2\rangle$

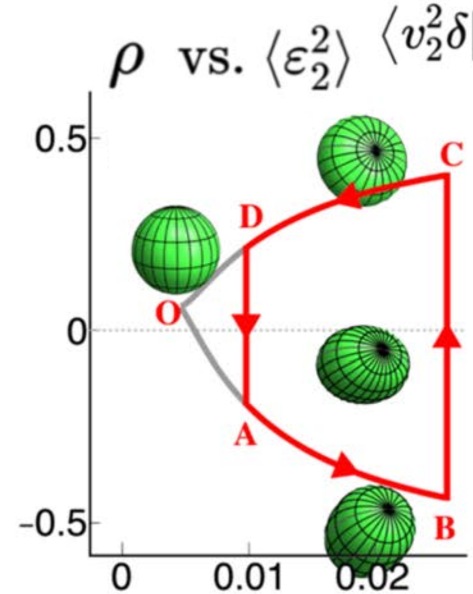

Collision system scan to map out this trajectory: calibrate coefficients with species with known β,γ, then predict for species of interest.

Shape fluctuations

- Shape fluctuations and shape coexistence can be accessed via high-order correlations

Shape coexistence

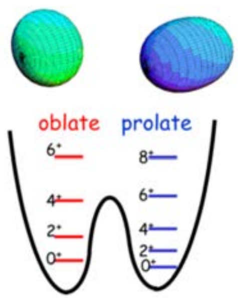

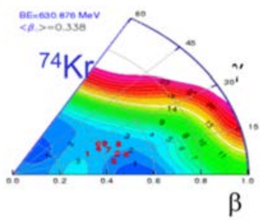

$$R = \frac{\left\langle v_2^2 \delta[p_T] \right\rangle_{^{129}Xe}}{\left\langle v_2^2 \delta[p_T] \right\rangle_{^{208}Pb}}$$

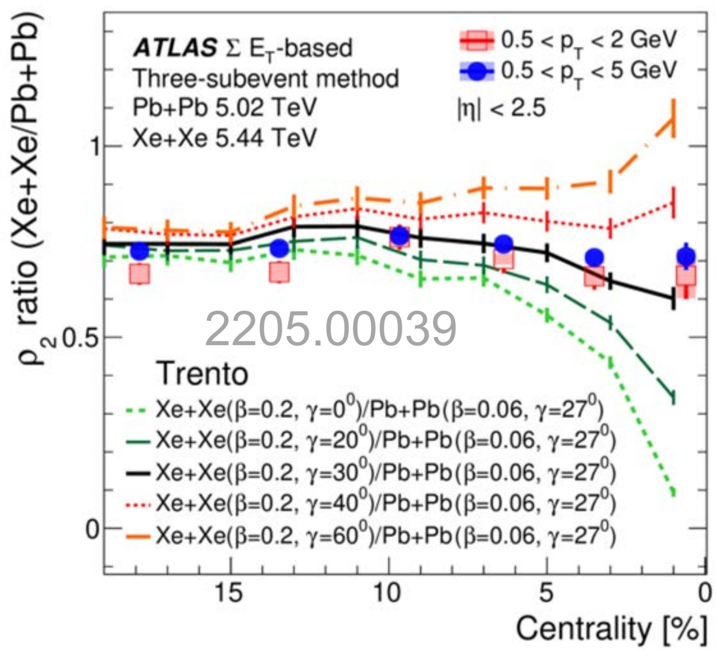

Bally et.al 2108.09578

Large shape fluct., esp along γ

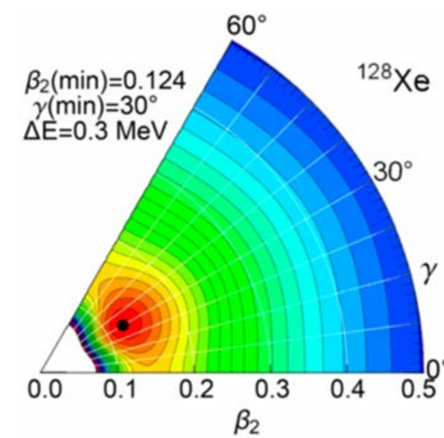

PhysRevC.101.064318

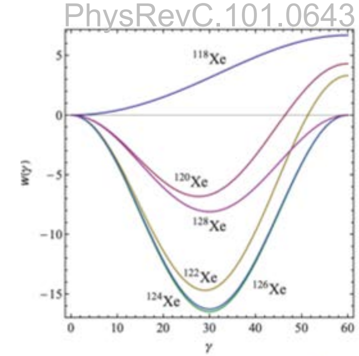

FIG. 3. The evolution of the γ potential defined by Eq. (7) with itted parameters c_1 and c_2, along the isotopic chain $^{118-128}$Xe.

Shape fluctuations

- Shape fluctuations and shape coexistence can be accessed via high-order correlations.

Shape coexistence

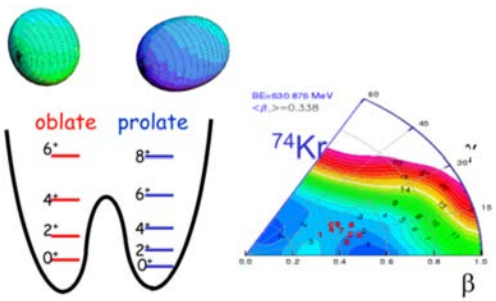

quadrupole operator $\hat{Q}$

$$\begin{cases} \langle \beta^2 \rangle = \dfrac{16\pi^2}{9A^2R_0^4}\left\langle \hat{Q}^2 \right\rangle & \text{2-p correlation} \\ \sigma^2(\langle \beta^2 \rangle)/\langle \beta^2 \rangle = \sigma^2\left(\langle \hat{Q}^2 \rangle\right)/\langle \hat{Q}^2 \rangle & \text{4-p correlation} \end{cases}$$

1906.07542

$$\begin{cases} \langle \cos 3\gamma \rangle = -\sqrt{\dfrac{7}{2}}\dfrac{\left\langle \hat{Q}^3 \right\rangle}{\left\langle \hat{Q}^2 \right\rangle^{3/2}} & \text{3-p correlation} \\ \dfrac{\sigma^2(\cos 3\gamma)}{(\cos 3\gamma)^2} = \dfrac{\sigma^2\langle \hat{Q}^3 \rangle}{\langle \hat{Q}^3 \rangle^2} + \dfrac{9}{4}\dfrac{\sigma^2\langle \hat{Q}^2 \rangle}{\langle \hat{Q}^2 \rangle^2} - 3\dfrac{\langle \hat{Q}^5 \rangle - \langle \hat{Q}^3 \rangle\langle \hat{Q}^2 \rangle}{\langle \hat{Q}^3 \rangle\langle \hat{Q}^2 \rangle} & \text{6-p correlation} \end{cases}$$

Heavy ion observables:

arXiv:2301.03556

$$\frac{\left\langle \varepsilon_2^2 \right\rangle}{\frac{3}{4\pi}\left\langle \beta_2^2 \right\rangle} \qquad \frac{\left\langle \varepsilon_2^4 \right\rangle - 2\left\langle \varepsilon_2^2 \right\rangle^2}{-\frac{9}{112\pi^2}\left(7\left\langle \beta_2^2 \right\rangle^2 - 5\left\langle \beta_2^4 \right\rangle\right)}$$

$$\frac{\left\langle \varepsilon_2^2(\delta d_\perp/d_\perp) \right\rangle}{-\frac{3\sqrt{5}}{112\pi^{3/2}}\left\langle \cos(3\gamma)\beta_2^3 \right\rangle} \qquad \frac{\left(\left\langle \varepsilon_2^6 \right\rangle - 9\left\langle \varepsilon_2^4 \right\rangle\left\langle \varepsilon_2^2 \right\rangle + 12\left\langle \varepsilon_2^2 \right\rangle^3\right)/4}{\frac{81}{256\pi^3}\left[\left\langle \beta_2^2 \right\rangle^3 - \frac{45}{14}\left\langle \beta_2^4 \right\rangle\left\langle \beta_2^2 \right\rangle - \frac{1175}{6006}\left\langle \beta_2^6 \right\rangle + \frac{25}{3003}\left\langle \cos(6\gamma)\beta_2^6 \right\rangle\right]}$$

Shape fluctuations

Fluctuation in γ washes out difference between prolate and oblate, such that all results approach triaxial case

$$\langle \cos(3\gamma) \rangle \approx e^{-\frac{9\sigma_\gamma^2}{2}} \cos\left(3\bar{\gamma} - \frac{9}{2} k_{3,\gamma}\right) \qquad \sigma_\gamma^2 = \langle (\gamma - \bar{\gamma})^2 \rangle \quad k_{3,\gamma} = \langle (\gamma - \bar{\gamma})^3 \rangle$$

Talk by Aman Dimiri

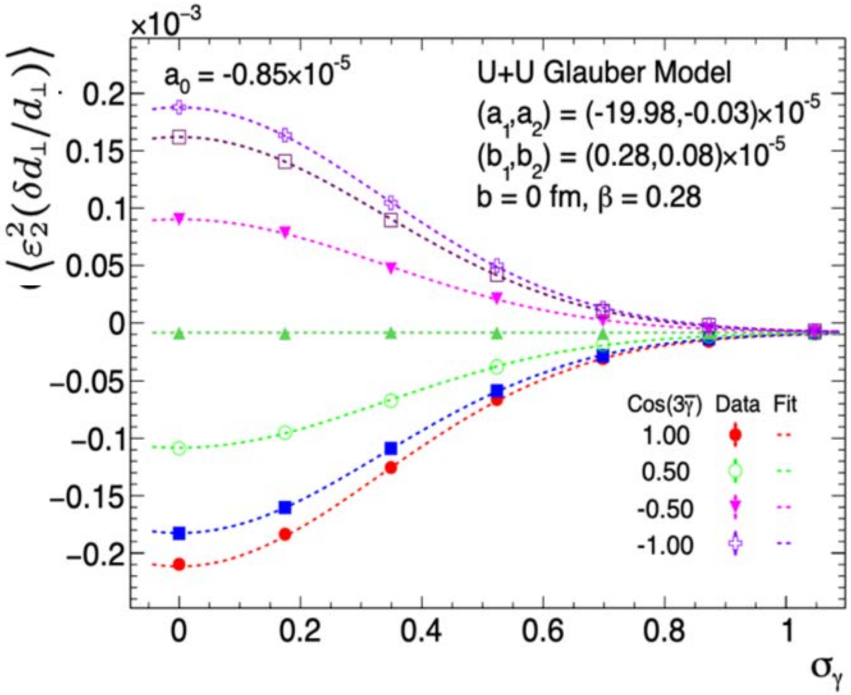

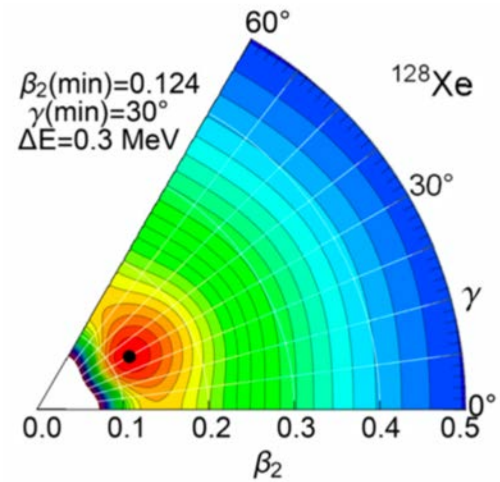

Neutron skin in high-energy collisions

PREX and CREX has tension with theory and previous exp. Indicate a larger L value.

$$\Delta r_{\mathrm{np,Pb}} = 0.28 \pm 0.07\mathrm{fm}$$
$$\Delta r_{\mathrm{np,Ca}} = 0.14 \pm 0.03\mathrm{fm}$$

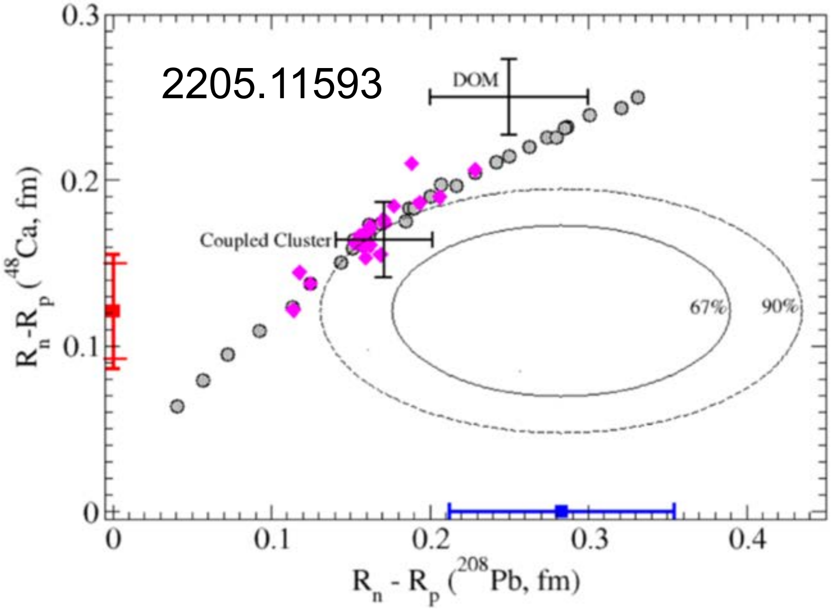

- Access the difference of neutron skin by comparing 40Ca+40Ca and 48Ca+48Ca

We know:

$$\sqrt{\langle r_{\mathrm{p}}^2\rangle}(^{48}\mathrm{Ca}) = \sqrt{\langle r_{\mathrm{p}}^2\rangle}(^{40}\mathrm{Ca})$$
$$\sqrt{\langle r_{\mathrm{p}}^2\rangle}(^{40}\mathrm{Ca}) \approx \sqrt{\langle r_{\mathrm{n}}^2\rangle}(^{40}\mathrm{Ca})$$

Hence :

$$\Delta_{\mathrm{np}}(^{48}\mathrm{Ca}) - \Delta_{\mathrm{np}}(^{40}\mathrm{Ca}) \simeq \Delta_{\mathrm{np}}(^{48}\mathrm{Ca})$$
$$\propto \bar{R}_0 \Delta R_0 + 7/3\pi^2 \bar{a} \Delta a$$

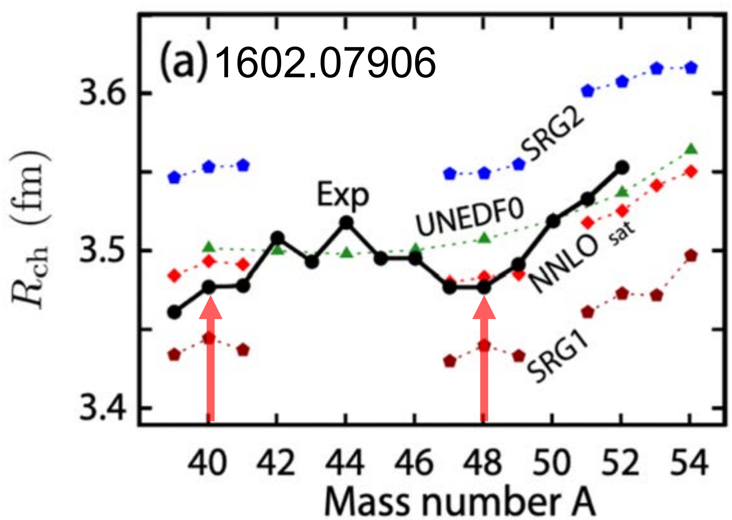

Directly peeling off the skin matter

- Similar to low energy fragmentation reaction

Andrea Jedele

TECHNISCHE UNIVERSITÄT DARMSTADT NuSym2021

$$\boxed{\sigma_R} = \sigma_R^{\mathrm{NN}} + \sigma_R^{coll}$$

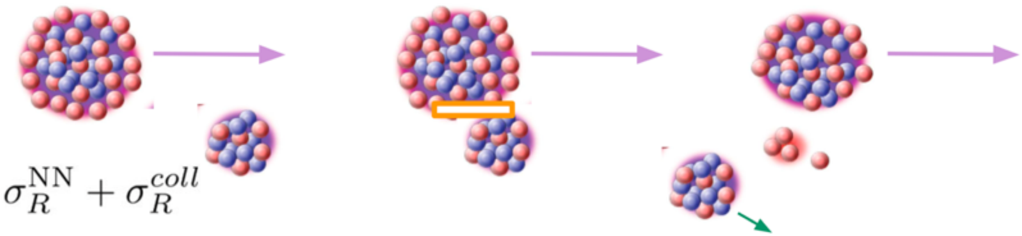

- Spectator neutrons in ultra-central isobar collisions is enhanced by neutron skin

N.Kozyrev, I. Pshenichnov 2204.07189

L. Liu, J. Xu et.al 2203.09924

Complete separation between participant and spectator matter

Talk by Lumeng Liu

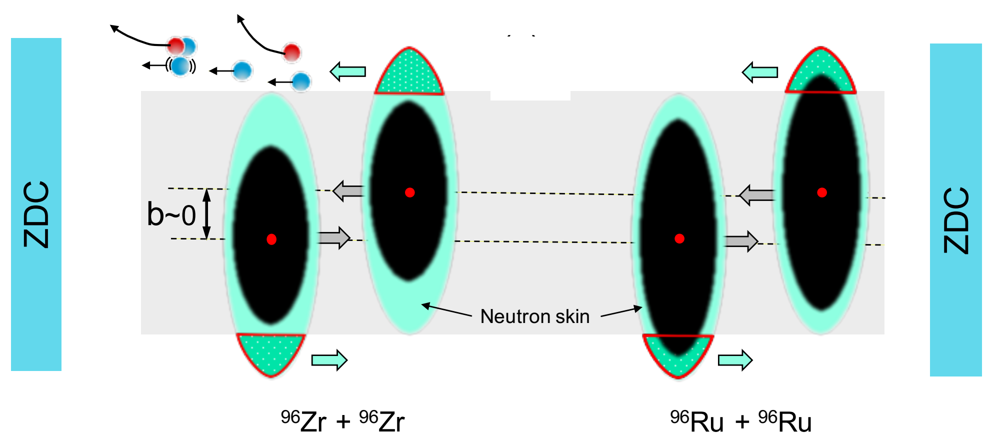

Summary

- Constrain QGP initial condition with nuclear structure input
  ➔ Improve the extraction of QGP properties in the Bayesian approaches
- Understanding how initial condition responds to nuclear structure, in turn probes novel nuclear structure properties and add to low-energy studies.
- Collisions of carefully-selected isobar species (at LHC) will help us to understand the many-body nucleon correlations of atomic nuclei from small to large system

work are needed to firm-up this science case

A	isobars	A	isobars	A	isobars	A	isobars	A	isobars	A	isobars
36	Ar, S	80	Se, Kr	106	Pd, Cd	124	Sn, Te, Xe	148	Nd, Sm	174	Yb, Hf
40	Ca, Ar	84	Kr, Sr, Mo	108	Pd, Cd	126	Te, Xe	150	Nd, Sm	176	Yb, Lu, Hf
46	Ca, Ti	86	Kr, Sr	110	Pd, Cd	128	Te, Xe	152	Sm, Gd	180	Hf, W
48	Ca, Ti	87	Rb, Sr	112	Cd, Sn	130	Te, Xe, Ba	154	Sm, Gd	184	W, Os
50	Ti, V, Cr	92	Zr, Nb, Mo	113	Cd, In	132	Xe, Ba	156	Gd,Dy	186	W, Os
54	Cr, Fe	94	Zr, Mo	114	Cd, Sn	134	Xe, Ba	158	Gd,Dy	187	Re, Os
64	Ni, Zn	96	Zr, Mo, Ru	115	In, Sn	136	Xe, Ba, Ce	160	Gd,Dy	190	Os, Pt
70	Zn, Ge	98	Mo, Ru	116	Cd, Sn	138	Ba, La, Ce	162	Dy,Er	192	Os, Pt
74	Ge, Se	100	Mo, Ru	120	Sn, Te	142	Ce, Nd	164	Dy,Er	196	Pt, Hg
76	Ge, Se	102	Ru, Pd	122	Sn, Te	144	Nd, Sm	168	Er,Yb	198	Pt, Hg
78	Se, Kr	104	Ru, Pd	123	Sb, Te	146	Nd, Sm	170	Er,Yb	204	Hg, Pb

TABLE I. Pairs and triplets of stable isobars (half-life $> 10^8$ y). 141 nuclides are listed. The region marked in red contains large strongly-deformed nuclei ($\beta_2 > 0.2$). The region marked in blue corresponds to nuclides which may present an octupole deformation in their ground state [48].